



Universiteit
Leiden
The Netherlands

Modulation of plant chemistry by rhizosphere bacteria

Jeon, J.

Citation

Jeon, J. (2020, July 7). *Modulation of plant chemistry by rhizosphere bacteria*. NIOO-thesis. Retrieved from <https://hdl.handle.net/1887/123229>

Version: Publisher's Version

License: [Licence agreement concerning inclusion of doctoral thesis in the Institutional Repository of the University of Leiden](#)

Downloaded from: <https://hdl.handle.net/1887/123229>

Note: To cite this publication please use the final published version (if applicable).

Cover Page



Universiteit Leiden



The handle <http://hdl.handle.net/1887/123229> holds various files of this Leiden University dissertation.

Author: Jeon, J.

Title: Modulation of plant chemistry by rhizosphere bacteria

Issue Date: 2020-07-07

Chapter 4

Steering the Broccoli shoot metabolome by root-colonizing *Paraburkholderia* species: impacts on growth and defense

Je-Seung Jeon, Natalia Carreno-Quintero, Ric De Vos,
Jos M. Raaijmakers and Desalegn W. Etalo

Manuscript submitted for publication

Abstract

Beneficial rhizobacteria can promote plant growth and induce resistance. Recent advances in analytical chemistry allow to study the impact of rhizobacteria on primary and secondary metabolism in plants and how these changes associate with the plant phenotypic changes. In this study, a new strategy integrating GC/LC-MS-based metabolomics was firstly employed to elucidate changes in primary and secondary metabolite networks in the shoots of two Broccoli cultivars upon root colonization by three *Paraburkholderia* species, *P. graminis* (*Pbg*), *P. hospita* (*Pbh*), and *P. terricola* (*Pbt*). Results showed that *Pbt* was a poor colonizer of the roots of Malibu cultivar and did not promote plant growth in contrast to other combinations of the two Broccoli cultivars and *Paraburkholderia* species. *Pbh* and *Pbt* induced resistance in Malibu cultivar to infections by the bacterial leaf pathogen *Xanthomonas campestris*. Subsequent metabolomics exhibited that soluble sugar levels were much higher in leaves of Malibu cultivar most likely providing resources for the biosynthesis of phenylpropanoid downstream metabolites such as hydroxycinnamates, flavonoids, and stilbenoids, metabolites with antimicrobial activities. In addition to enhancement of key precursors for growth and secondary metabolite biosynthesis, treatment of *Paraburkholderia* also induced metabolite remobilization. The metabolite remobilization involved both suppression of resource competing metabolite pathways such as amino acids and rechanneling of existing primary metabolite-derivatives and other secondary metabolites to other metabolite pathways. Flavonoids, hydroxycinnamates, stilbenoids, coumarins and lignins showed substantial accumulation upon treatments with the *Paraburkholderia* species, metabolites with direct antimicrobial effects and that can act as a physical barrier against pathogenic bacteria such as *Xanthomonas campestris*. The integrated primary and secondary metabolome profiling conducted in this study further suggests that rhizobacteria could avert the negative impact of defense priming on the host fitness by generating substantial amounts of soluble sugars and by remobilizing other metabolites to compensate for the high energy and carbon skeleton demand associated with growth and defense priming.

Keywords: broccoli metabolites; *Paraburkholderia*; beneficial rhizobacteria; non-targeted metabolomics; secondary metabolites, primary metabolites.

Introduction

Plants are fine-tuned factories of more than 100,000 secondary metabolites (Wink, 2010). Many plant species exhibit pharmaceutical activities, providing valuable scaffolds for the development of new pharmaceuticals (Cragg & Newman, 2013; Bauer & Brönstrup, 2014). For the plant itself, secondary metabolites are involved in adaptation to environmental changes (Bourgaud *et al.*, 2001) including tolerance to biotic stresses such as insect herbivory and pathogen infections (Bennett & Wallsgrove, 1994; Rattan, 2010; Boulogne *et al.*, 2012). Therefore, steering plant chemistry to elevate specific metabolites has been a major direction in plant breeding. Recent studies have shown that rhizobacteria, i.e. bacteria colonizing the surface and internal plant root tissue, can enhance plant growth, induce systemic resistance and alter changes in plant chemistry, providing new avenues to enhance the levels of specific plant secondary metabolites of interest.

Plants photosynthetically fix carbon and metabolize it for growth and defense. Both processes appear incompatible due to limited resources and is referred to as the “defense-growth trade-off” (Huot *et al.*, 2014). However, several studies have shown that specific rhizobacteria can parallelly induce both growth and defense. For instance, our previous studies demonstrated that *Pseudomonas fluorescens* SS101 enhanced biomass of *Arabidopsis* as well as resistance against a bacterial leaf pathogen and insect herbivory (van de Mortel *et al.*, 2012; Cheng *et al.*, 2017). Similar results were observed in *Oryza sativa* (Chamam *et al.*, 2013), *Panax ginseng* (Gao *et al.*, 2015), *Piper betle* (Lavania *et al.*, 2006), *Pisum sativum* (Mabrouk *et al.*, 2007), and *Salvia officinalis* (Ghorbanpour *et al.*, 2016) upon inoculation with various rhizobacterial genera. However, how specific rhizobacteria induce defense and enhance growth simultaneously is not well understood. Here, we studied the impact of root-colonizing *Paraburkholderia* species on growth and defense of two Broccoli cultivars. Broccoli (*Brassica olearacea* var. *italica*) is a crop plant consumed worldwide, known to have high value natural compounds including glucosinolates and flavonoids (Naguib *et al.*, 2012). The Broccoli cultivars used in present study were Coronado and Malibu, bred to possess high and lower levels of glucosinolates (glucoiberin, glucoraphanin and glucobrassicin), respectively. *Paraburkholderia* is a diverged monophyletic clade from the genus *Burkholderia* (Sawana *et al.*, 2014). A number of rhizospheric and endophytic *Paraburkholderia* species, in particular *Paraburkholderia phytofirmans* PsJN, *P. fungorum* and *P. graminis*, can promote growth of maize, strawberry and *Arabidopsis* (Ledger *et al.*, 2016; Mitter *et al.*, 2017; Rahman *et al.*, 2018) and suppress pathogen infections (Timmermann *et al.*, 2017; Carrión *et al.*, 2018). Also various *Paraburkholderia* species are typically found in the mycosphere consuming organic acids released from the fungi and using the hyphae as ‘highways’ for translocation (Nazir *et al.*, 2009). The *Paraburkholderia* species used in our work presented here are *Paraburkholderia graminis* (Pbg), *P. hospita* (Pbh), and *P. terricola* (Pbt) which exhibited plant protection against the fungal root pathogen *Rhizoctonia solani*. For *P. graminis*, we further showed that the production of sulfurous volatiles was a key mechanism in disease

suppression (Carrión *et al.*, 2018).

In the present study, we monitored the effects of different root-colonizing *Paraburkholderia* species on phenotypes of two Broccoli cultivars, in particular growth promotion and defense against the bacterial leaf pathogen *Xanthomonas campestris*. At two different time points during the *Paraburkholderia*-Broccoli interactions we conducted untargeted metabolomics to map the systemic changes in primary and secondary metabolism in the shoots of Broccoli. Our results show that, in the partnerships of *Paraburkholderia* species with the two Broccoli cultivars, there were common and specific signatures in both primary and secondary metabolism. The results suggest that the enhanced accumulation of soluble sugars in shoots of Broccoli cultivars upon *Paraburkholderia* root colonization translate into distinct changes in secondary metabolism that in turn associate with distinctive changes in plant growth and defense. The integrated strategy adopted in this study enhanced our fundamental understanding of metabolic fluxes associated with plant growth and defense.

Materials and Methods

Bacterial strains and culture conditions

The rhizobacterial strains *Paraburkholderia graminis* (*Pbg*), *P. hospita* (*Pbh*), and *P. terricola* (*Pbt*) used in this study were originally isolated from rhizospheric soil of *Beta vulgaris* grown in *Rhizoctonia solani* suppressive soil (Carrión *et al.*, 2018). Culture of *Paraburkholderia* species were maintained in Luria Bertani (LB)-medium (Lennox, Carl Roth) at 25 °C. After incubation for 16 hours, bacteria cells were spun down to make bacteria pellets. These pellets were then washed three times with 10 mM MgSO₄ and resuspended in 10 mM MgSO₄ to a final density of OD₆₀₀ = 1.0 (~10⁹ cells per ml).

Plant Materials and growth conditions

Seeds of two Broccoli cultivars (*Brassica olearacea* var. *italica*), Coronado and Malibu, were kindly provided by Bejo Seeds (Warmenhuizen, The Netherlands). The seeds were surface sterilized for 30 minutes by immersing them in 1% (v/v) sodium hypochlorite amended with 0.1 % (v/v) of Tween 20, and rinsed three times with ample sterile distilled water. Thereafter, five seeds were sown on 100 X 100 mm square petri dishes containing 50 ml of half-strength Murashige and Skoog (0.5 X MS) agar media with 0.5% sucrose (w/v) and 1.2% plant agar (w/v). Five days after germination and vegetative growth in petri dishes, the root tips of the seedlings from the two Broccoli cultivars were inoculated with 2 µl cell suspension (±10⁹ cells per ml) of each three *Paraburkholderia* species. Plants treated with 2 µl 10 mM MgSO₄ served as controls. The plates with the control and inoculated plants were then sealed and incubated in a climate chamber (21 °C / 21 °C day/night temperature; 180 µmol light m⁻²s⁻¹ at plant level during 16 h/d; 70% relative humidity) until harvest (11 days post inoculation).

Temporal changes in shoot fresh biomass were measured every two days until harvest.

Rhizobacteria root colonization assay

Bacterial root colonization was determined at 6 and 11 dpi for each of the three *Paraburkholderia* species on each of the two Broccoli cultivars. Briefly, treated roots were collected at 6 and 11 dpi and placed in sterile 50 mL Falcon tube and its biomass was measured. Then the root samples were vortexed (60 s) in 10 mM MgSO₄, sonicated (60 s), and again vortexed (15 s) to resuspend the bacteria adhering to the root. The suspensions were serial dilution plated onto PSA plates containing 100 µg ml⁻¹ delvodic (DSM) to inhibit fungal growth. Plates were incubated at 25 °C in the dark for 3 days, colonies were counted and the number of colony-forming units (cfu) per gram of root fresh weight was calculated.

Plant phenotyping

Fresh biomass of the Broccoli shoots was measured to determine the effect of the rhizobacteria on plant growth. For Broccoli, shoot fresh biomass from the respective treatments was weighed every two day after bacterial inoculation until the last harvest at 11 dpi. The average weight of 5 Broccoli seedlings was considered as one independent biological replicate. The roots were carefully removed from the MS-agar and washed with distilled water to eliminate adhering agar, blotted dry on filter paper and their fresh weight was recorded.

Induced resistance assays

To assess the impact of *Paraburkholderia* species on induced resistance, the two Broccoli cultivars were inoculated with the three *Paraburkholderia* species and grown for 11 days. Thereafter, leaves were inoculated with the bacterial leaf pathogens *Xanthomonas campestris* pv. *Aarmoraciae* P4216 (*Xca*) and *Xanthomonas campestris* pv. *Campestris* P4014 (*Xcc*). To do that, *Xca* and *Xcc* were cultured in LB-medium at 25 °C. After 16 hours, bacterial cells were washed following similar procedure for *Paraburkholderia* as described above. A 2 µl suspension of *Xca* or *Xcc* (~1 X 10⁹ cell per ml) was inoculated on the first true leaf of the Broccoli seedlings after scratching the leaf surface with sterile 20 µl pipet tips. Ten days after pathogen challenge, disease severity of the shoots was assessed by determining the migration of the lesion from the inoculation spot to the other parts of the shoot following an ordinal scale from 0 - 5 as shown in supplementary **Fig S2**. Severity values were converted to 0 to 100 Disease severity index (DSI) using the equation (Kobriger & Hagedorn, 1983). DSI (%) = $\sum(\text{severity class} \times \text{no. plants in class}) / (\text{total no. of plants} \times \text{the highest class No.})$

Plant metabolomics

Sample collection

Shoots from the control plants and plants treated with three *Paraburkholderia* species were harvested at 6 and 11 dpi. For each plant cultivar x *Paraburkholderia* combination, 4 biological replicates of 5 plants each were considered. Briefly, shoots were snap frozen in liquid nitrogen and ground to fine powder under continuous cooling and kept at -80 °C until further use.

Polar primary metabolite extraction and analysis

Polar primary metabolite sample preparation was performed as described by (Weckwerth *et al.*, 2004; Carreno-Quintero *et al.*, 2012). Briefly, a total of 1.4 mL of methanol containing ribitol (0.2mg/mL) as an internal standard was added to a 2 mL Eppendorf tube containing a total of 200 mg Broccoli leaf powder. After vortexing (10 s) and shaking in a thermomixer at 950 rpm for 10 min, the samples were centrifuged at maximum speed for 10 min. 500 μ L of the supernatant was transferred to a new 2 mL Eppendorf tube and 370 μ L of chloroform and 750 μ L of distilled water were added. The mixture was vigorously mixed by vortexing and centrifuging for 10 min at maximum speed (14,000 rpm). 50 μ L of the upper polar phase was transferred to an insert in a 2 mL vial. The solvent was then vacuum dried (speedvac) for 16 h at room temperature and sealed under an argon atmosphere. The dried samples were derivatized online as described by Lisec *et al.* (2006) using a Combi PAL autosampler (CTC Analytics). Initially, 12.5 μ L methoxyamine (20 mg mL⁻¹ pyridine) was added to each of the samples and incubated for 30 min at 40 °C under agitation. The samples were then derivatized for one hour by adding 17.5 μ L of *N*-methyl-*N*-(trimethylsilyl) trifluoroacetamide (MSTFA). An alkane mixture (C11-C21 and C24-C33) was added to determine the retention indices of metabolites. The derivatized samples were analyzed by a GC-TOF-MS system consisting of an Optic 3 high-performance injector (ATAS) and an Agilent 6890 gas chromatograph (Agilent Technologies) coupled to a Pegasus III time-of-flight mass spectrometer (Leco Instruments).

2 μ L of each sample was subjected to the injector at 70 °C using a split flow of 19 mL min⁻¹. The chromatographic separation was performed using a VF-5ms capillary column (Varian; 30 m x 0.25 mm x 0.25 mm) including a 10-m guardian column with helium as carrier gas at a flow rate of 1 mL min⁻¹. The temperature was isothermal for 2 min at 70 °C, followed by a 10 °C min⁻¹ ramp to 310 °C, and was held for 5 min. The transfer line temperature was set at 270 °C. The column effluent was ionized by electron impact at 70 eV. Mass spectra were acquired at 20 scans s⁻¹ within a mass-to-charge ratio range of 50 to 600 at a source temperature of 200 °C. A solvent delay of 295 s was set. The detector voltage was set to 1,400 V.

Semi-polar secondary metabolite extraction and analysis

For extraction of semi-polar secondary metabolites, 300 μL of 99.89% methanol containing 0.13% (v/v) formic acid was added to 100 mg plant material in 2 ml round bottom Eppendorf tubes, and sonicated for 15 min followed by centrifugation for 15 min at 20,000 X g. The supernatants containing predominantly the semi-polar metabolites were transferred to 96-well filter plate (AcroPrepTM, 350 μL , 0.45 μm , PALL), vacuum filtrated to the 96-deep-well autosampler plates (Waters) using a Genesis Workstation (Tecan Systems).

An UltiMate 3000 U-HPLC system (Dionex) was used to create a 45 minutes linear gradient of 5-35% acetonitrile in 0.1% formic acid (FA) in water at a flow rate of 0.19 ml min⁻¹. 5 μl of each extract was injected and compounds were separated on a Luna C18 column (2.0 X 150 mm, 3 μm ; Phenomenex) maintained at 40 °C (De Vos *et al.*, 2007). The detection of compounds eluting from the column was performed with a Q-Exactive Plus Orbitrap FTMS mass spectrometer (Thermo Scientific). Full scan MS data were generated with electrospray in switching positive/negative ionization mode at a mass resolution of 35,000 (FWHM at m/z 200) in a range of m/z 95-1350. Subsequent MS/MS experiments for identification of selected metabolites were performed with separate positive or negative electrospray ionization at a normalized collision energy of 27 and a mass resolution of 17,500. The ionization voltage was optimized at 3.5 kV for positive mode and 2.5 kV for negative mode; capillary temperature was set at 250 °C; the auxiliary gas heater temperature was set to 220 °C; sheath gas, auxiliary gas and the sweep gas flow were optimized at 36, 10 and 1 arbitrary units, respectively. Automatic gain control was set a 3⁶⁶ and the injection time at 100 ms. External mass calibration with formic acid clusters was performed in both positive and negative ionization modes before each sample series.

Data processing and analysis

GC-TOF-MS

Raw data was primarily processed by Chroma TOF software 2.0 (Leco Instruments) and MassLynx software (Waters), and subjected to MetAlign software to extract and align the mass signal whose signal-to-noise ratio larger than 3 as described by Carreno-Quintero *et al.* (2012). The mass features were considered as a signal if they were detected in at least 3 biological replicates. Mass features fragments originating from the same metabolites were clustered together by MSclust software into 138 representative primary metabolites. Further, data transformation and scaling were performed in GeneMaths XT 1.6 (www.applied-maths.com). This then used for hierarchical cluster analysis using Pearson's correlation coefficient and Unweighted Pair Group Method with Arithmetic Mean (UPGMA). To identify metabolites, the reconstructed mass spectra file was introduced to NIST MS search software (v 2.2) with Wiley spectral libraries and in-house library, followed by comparison with

retention indices determined by a series of alkanes. Metabolite annotations were manually curated. The mass intensity of the representative metabolites was normalized by the internal standard, ribitol.

LC-MS

Peak picking, baseline correction, and mass signal alignment of the LC-MS data was performed using Metalign software (Lommen, 2009). The mass features were considered as a signal if they were detected in at least 3 biological replicates of a treatment with signal intensity 3 times of the noise value. Then, mass features originating from the same metabolites were clustered based on retention window and their correlation across all measured samples, using MSClust software (Tikunov *et al.*, 2012). After this, so-called centrotypes, representing reconstructed putative metabolites mass spectra were selected, of which relative abundance was represented by the Measured Ion Count (MIC) representing the sum of the ion count values (corrected by their membership) for all measured cluster ions in a given sample. The samples were batch corrected to reduce batch effect of large series of samples during the LCMS analysis according to (Wehrens *et al.*, 2016). ANOVA and fold changes > 2.0 were applied to identify mass signals that were significantly changed between the treatments. Data transformation and scaling was performed in GeneMaths XT 1.6 (www.applied-maths.com). Transformed and scaled values were used for hierarchical cluster analysis using Pearson's correlation coefficient and Unweighted Pair Group Method with Arithmetic Mean (UPGMA).

Annotation of differential metabolites was performed based on selection of pseudomolecule ions from the masses in the MSClust-reconstructed metabolites, first by matching their accurate masses plus retention times to previously reported metabolites present in Arabidopsis and Broccoli on the same LC-MS system and similar chromatographic conditions. Second, if compounds were not yet present in this experimentally obtained database, detected masses were matched with compound libraries, including Metabolomics Japan (www.metabolomics.jp), the Dictionary of Natural Products (<http://dnp.chemnetbase.com>), KNApSAcK (<http://kanaya.naist.jp/KNApSAcK>), and Metlin (<http://metlin.scripps.edu/>) using a maximum deviation of observed mass from calculated of 5 ppm. The identity of potential candidate metabolites was further verified using Magma online tool (Ridder *et al.*, 2013) that compares the InSilco fragmentation patterns of a given metabolites to the experimentally obtained fragmentation patterns.

Statistical analysis

The relative changes in shoot biomass, root biomass in the combinations of two Broccoli cultivars and *Paraburkholderia* species was analyzed with R Studio software (Version 3.6.1). First, the normality and homogeneity of variance of the data was assessed and when the two assumptions were not met the data was transformed using Box-Cox or log transformation

using a package MASS. Differences were tested by two-way analysis of variance (ANOVA). A Tukey-HSD test was used to separate group mean values when the ANOVA was significant at $p < 0.05$. The ANOVA table is shown in Supplementary Material, **Table S1**. Differences in phenotypic parameters between the rhizobacterial treatments and non-treated controls were assessed by Student's t -Test.

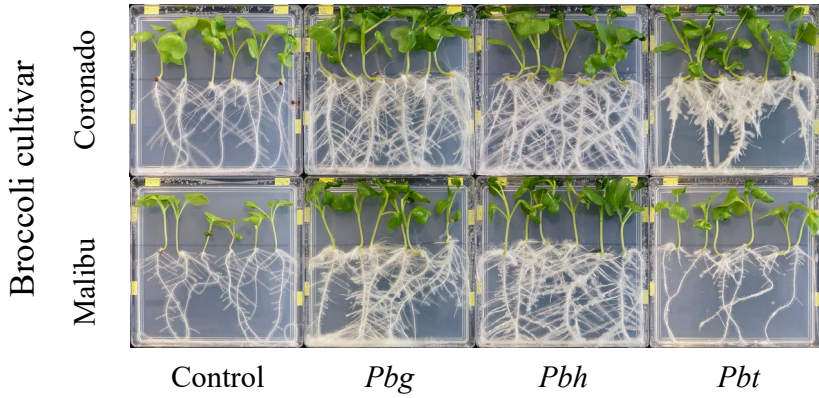
Results

Paraburkholderia species promote growth of Broccoli

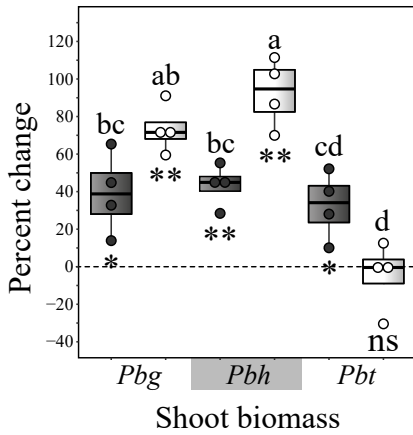
In general, root tip inoculation of the Broccoli cultivars with different *Paraburkholderia* species led to changes in leaf color (deep green leaves), shoot biomass, root biomass and root architecture (**Fig 1a**). Percent change in biomass was used as a standard measure to assess the growth-promoting effects of the *Paraburkholderia* species in two Broccoli cultivars. The percent change in biomass was calculated by dividing the biomass difference between rhizobacteria-treated plants and the control to the biomass of the control plants. Two-way analysis of variance was conducted to assess the influence of the two independent variables (*Paraburkholderia* species and Broccoli cultivars) on shoot and root biomass. The *Paraburkholderia* species included three levels (*Pbg*, *Pbh* and *Pbt*) and the Broccoli cultivars consisted of two levels (Coronado and Malibu). Furthermore, two-tailed student's t -test was used to assess the impact of the *Paraburkholderia* species inoculation on shoot and root biomass when compared to the control plants.

Results showed that all but *Pbt*-Malibu interaction resulted in significant increase in shoot biomass when compared to the control plants (**Fig 1b**). All three *Paraburkholderia* species significantly increased the root biomass in both Broccoli cultivars when compared to the control (**Fig 1c**). In general, the relative impact of *Paraburkholderia* species was up to 3 times higher for root biomass than for shoot biomass (**Fig 1b** and **1c**). The two-way ANOVA showed highly significant interactions between *Paraburkholderia* species and Broccoli cultivars regarding the percent change in shoot and root biomass (Supplementary **Table S1**). Overall, for cultivar Coronado the percent change in shoot biomass was not significantly different between the three *Paraburkholderia* species. Whereas, in Malibu the percent change in shoot biomass was significantly higher for *Pbg* and *Pbh* inoculated plants as compared to *Pbt*. Furthermore, inoculation of plants with *Pbh* led to a significantly higher increase in shoot biomass in Malibu than in cultivar Coronado. When it comes to percent change in root biomass, only inoculation of *Pbt* showed significant differences between the two Broccoli cultivars. Over a period of 11 days, both *Pbg* and *Pbh* inoculated Broccoli cultivars showed significantly higher shoot and root biomass from 7 dpi onwards. Whereas, *Pbt* inoculated plants showed significantly higher shoot biomass in Coronado cultivar from 9 dpi onward. As indicated above, the shoot biomass of Malibu cultivar inoculated with *Pbt* was not significantly different from the untreated plants (**Fig 1d**).

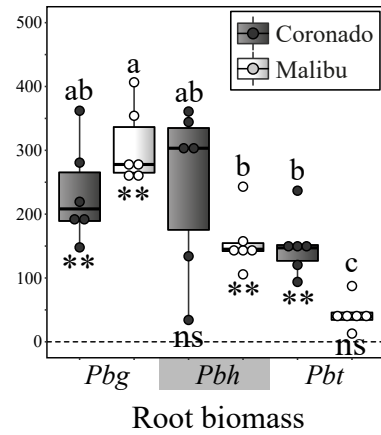
a



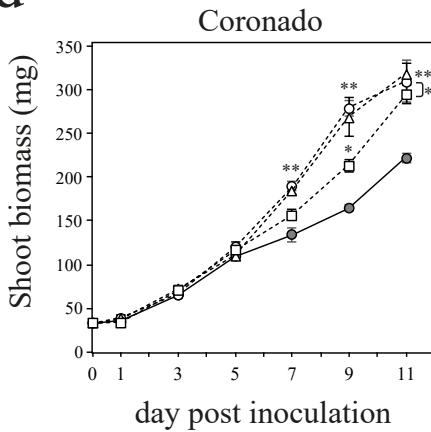
b



c



d¹



d²

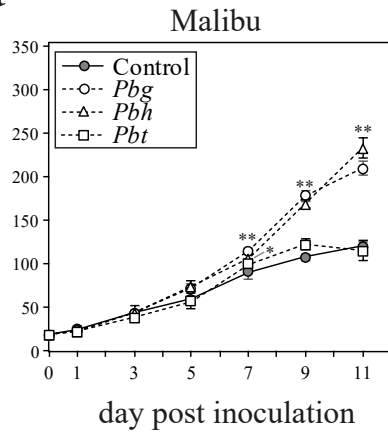


Fig 1.

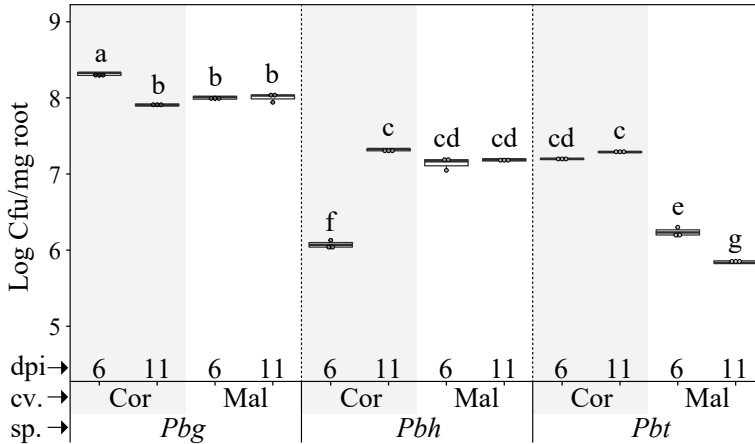


Fig 2. Root colonization ability of three *Paraburkholderia* species on two Broccoli cultivars at 6 and 11 dpi. Means of 3 replicates are shown. Different letters indicate significant differences based on three-ways ANOVA (Broccoli cultivars and Bacteria species, $P < 0.05$). Broccoli cultivars (Cor: Coronado, Mal: Malibu) and *Paraburkholderia* species, *Pbg*: *Paraburkholderia graminis*, *Pbh*: *P. hospita*, and *Pbt*: *P. terricola*.

Relation between root colonization and plant growth promotion

Root colonization of the three *Paraburkholderia* species was assessed for the two Broccoli cultivars at the early and late seedling growth stages. The data was log-transformed as the data did not meet both criteria for homogeneity of variance and normality. Three-way analysis of variance was conducted on the interaction effect of *Paraburkholderia* species, Broccoli cultivars and time after inoculation on root colonization. The *Paraburkholderia* species included three levels (*Pbg*, *Pbh* and *Pbt*), the Broccoli cultivars included two levels (Coronado and Malibu) and time after inoculation consisted of two levels (6 dpi and 11 dpi). There was highly significant three-way interaction effect on root colonization

◀◀◀ **Fig 1.** Biomass and phenotypic changes in Broccoli cultivars in response to root tip inoculation with three *Paraburkholderia* species. (a) Pictures of MS agar plate with two Broccoli cultivars (Coronado and Malibu) at 11 days post inoculation with the three *Paraburkholderia* species. (b) Percent changes in shoot biomass (mean \pm standard error, $n = 4$) and (c) Percent changes in root biomass (mean \pm standard error, $n = 6$) of two broccoli cultivars inoculated with the *Paraburkholderia* species. *Pbg*: *Paraburkholderia graminis*, *Pbh*: *P. hospita*, and *Pbt*: *P. terricola*. Different letters show significant difference between the treatments (Two-way ANOVA, Tukey's HSD *post hoc* test, $P < 0.05$). Asterisks denote statistical differences between non-bacteria treated control (two-tailed Student's t test): * $P < 0.05$; ** $P < 0.01$. (d) Temporal changes in shoot biomass of two Broccoli cultivars (d¹: Coronado and d²: Malibu) inoculated with the *Paraburkholderia* species. Asterisks denote statistical differences (two-tailed Student's t test): * $P < 0.05$; ** $P < 0.01$. *Pbg*: *Paraburkholderia graminis*, *Pbh*: *P. hospita*, and *Pbt*: *P. terricola*.

(Supplementary **Table S3**). In general, compared to the other two *Paraburkholderia* species, *Pbg* showed significantly higher root colonization in both cultivars at both time points (**Fig 2**) In addition, *Pbg* showed significantly higher root colonization in Coronado cultivar at early time point, while in Malibu the root colonization by *Pbg* was not significantly different between the two time points. In contrast, *Pbh* showed significantly lower root colonization at 6 dpi on Coronado cultivar. However, at the later time point, it showed significant increase in root colonization. Whereas, its root colonization was not significantly different between the two time points in Malibu cultivar. On the other hand, *Pbt* showed significantly lower root colonization in Malibu cultivar at both time points. Furthermore, *Pbt* on Malibu showed significant decline in root colonization at the later time point. Hence, ineffective growth promotion in combination of Malibu-*Pbt* seemed to have a strong correlation with cultivar specific lower root colonization capacity of *Pbt*.

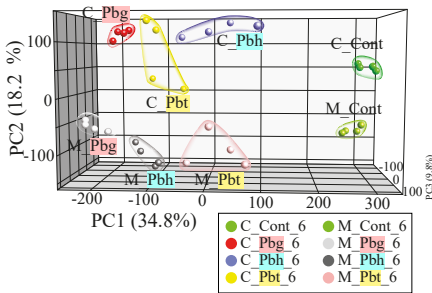
***Paraburkholderia* species altered primary and secondary metabolism of Broccoli shoot**

Considering the extent of species and cultivar-dependent variations in root colonization and plant growth promotion, we investigated the systemic effect of the different *Paraburkholderia* species on the shoot metabolome of the two Broccoli cultivars at 6 and 11 dpi. We specifically looked into the association between primary and secondary metabolism affected by the *Paraburkholderia* species. GC-MS- and LC-MS-based non-targeted metabolomics were used to profile polar primary metabolites and semi-polar secondary metabolites in shoot extracts, respectively. The data was subjected to ANOVA with correction for multiple testing (Benjamini-Hochberg) and metabolites that were significantly different ($P < 0.05$ and fold change >2) between at least two treatments were used for multivariate analysis. Principal Component Analysis (PCA) and Hierarchical Cluster Analysis (HCA) were used to reduce the dimensionality of the data and explore specific patterns between the different plant-rhizobacterial interactions.

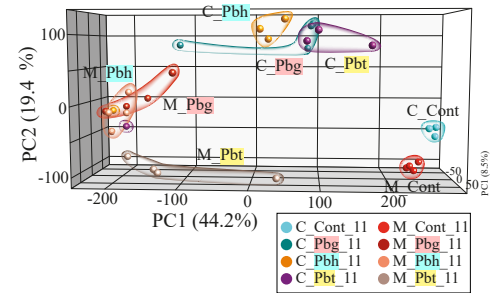
Effect of Paraburkholderia on shoot primary metabolism

GC-MS-based non-targeted metabolomics demonstrated that out of 138 polar metabolites, 68 metabolites were significantly different at least between two treatments in shoots of the two Broccoli cultivars upon inoculation with three rhizobacterial species at 6 and 11 dpi. At 6 dpi, PCA indicated that the first three principal components (PC) explained 67.7% of the total variance (**Fig 3a1**). The first PC (PC1), explained 34.8% of the total variance and corresponded to either enhanced or reduced metabolites in the Broccoli cultivars by the *Paraburkholderia* treatment when compared to the controls (**Fig 3b1**, Clusters **1, 5, 8** and **9**). Out of the three *Paraburkholderia* species, root tip inoculation by *Pbg* had the greatest impact on shoot primary metabolism of both Broccoli cultivars. Inoculation with *Pbh* and *Pbt* resulted in changes in the shoot primary metabolome in a cultivar-dependent manner. For *Pbh*, the impact on shoot primary metabolome was more extensive for Malibu than for

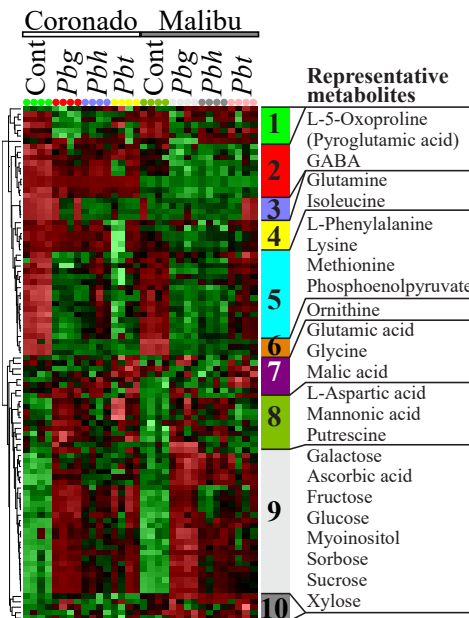
a1



a2



b1



b2

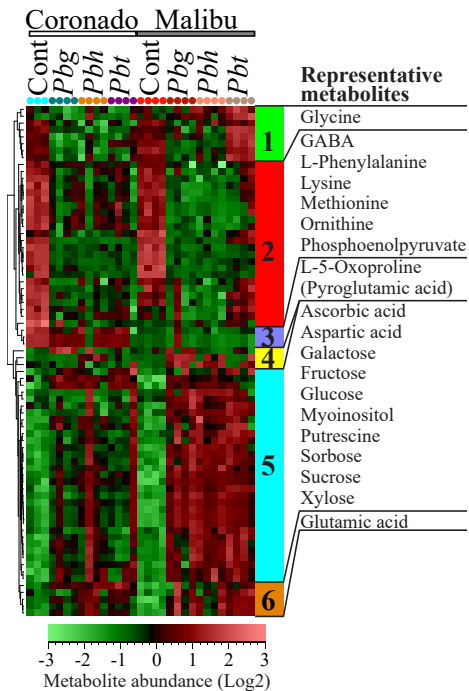


Fig 3. Rhizobacteria-mediated changes in shoot primary metabolites in two Broccoli cultivars. (a) Principal Component Analysis (PCA) and (b) Hierarchical Cluster Analysis (HCA) based on differentially regulated metabolites of the samples at 6 dpi (1) and 11 dpi (2). In the HCA, metabolite clusters are indicated by different colors. Information on the representative metabolites of each cluster is given on the right side, if the metabolites are annotated. (c) Impact of *Paraburkholderia* species on sugar generation and utilization of two Broccoli cultivars. Broccoli cultivars (Cor: Coronado, Mal: Malibu), Cont.: non-rhizobacteria treated control, *Pbg*: *Paraburkholderia graminis*, *Pbh*: *P. hospita*, and *Pbt*: *P. terricola*.

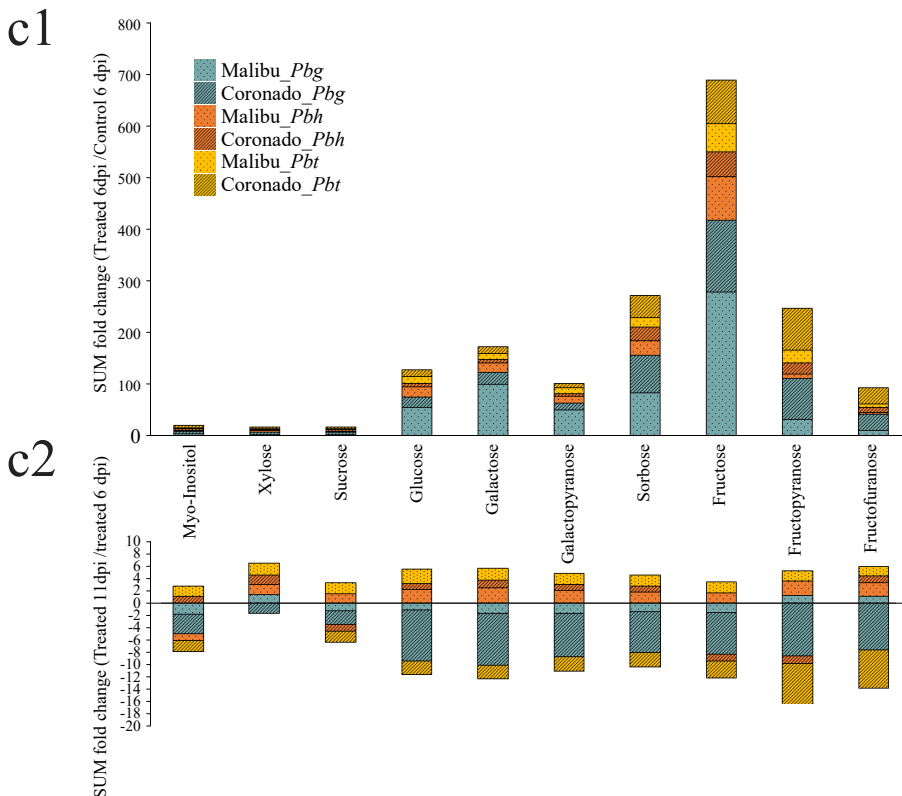


Fig 3. (continued)

Coronado, while for *Pbt* more extensive changes in the shoot primary metabolome were observed for Coronado (**Fig 3a1**). The major changes in primary metabolism induced by *Paraburkholderia* included accumulation of sugars (Cluster 9) and depletion of amino acids (Cluster 5, phenylalanine, lysine, methionine) and of the phosphate ester, phosphoenolpyruvate (PEP), a key intermediate in glycolysis and gluconeogenesis.

Some of the representative metabolites in cluster 8 that showed accumulation in all interactions, except in the ineffective *Pbt*-Malibu interaction, include aspartic acid, mannonic acid and putrescine. The second principal component (PC2) explained 18.2% of the total variance and associated with metabolites that showed variation between the two cultivars. Furthermore, treatment of the two cultivars with *Pbg* and *Pbh* widened the inherent variation in the level of some of the metabolites between the two Broccoli cultivars. (**Fig 3b1** Clusters 2 and 3). Amino acids such as glutamine, oxoproline (pyroglutamic acid), GABA (γ -aminobutyric acid) and isoleucine were intrinsically higher in Coronado when compared to Malibu.

At the later seedling growth stage (11 dpi), inoculation of the Broccoli cultivars with the three *Paraburkholderia* species continued to have substantial impact on shoot primary metabolism.

PCA showed that the first three principal component explained 72.0% of the total variance (**Fig 3a2**). Here, the impact of all three *Paraburkholderia* species on the shoot metabolome was Broccoli cultivar dependent and was greater in Malibu (**Fig 3a2**). The first principal component (PC1) explained 44.2% of the total variance and corresponded to metabolites that were enhanced (**Fig 3b2** Cluster 5) or reduced (Cluster 2) in the *Paraburkholderia* treatments. The depleted Broccoli shoot metabolites upon inoculation with the three rhizobacterial species encompassed amino acids such as lysine, phenylalanine, methionine, the non-proteinogenic amino acids ornithine and GABA, as well as the important metabolic intermediate phosphoenolpyruvate (PEP). In all but the ineffective partnership between *Pbt*-Malibu, the important intermediate phosphoenolpyruvate, showed 11-14 fold decreases (Supplementary excel, **Table S6**). On the other hand, sugars and other metabolites, including ascorbic acid and aspartic acid, represent the induced metabolites by the *Paraburkholderia* treatments when compared to the control plants (Cluster 5). Sugars showed greater abundance in Malibu cultivar treated with *Paraburkholderia* than in Coronado. However, at 11 dpi, sugars in *Paraburkholderia*-treated plants showed dramatic depletion in Coronado cultivar as compared to 6 dpi. Whereas in Malibu cultivar the temporal variation in the level of the sugars was less pronounced (**Fig 3b2** Cluster 5, Supplementary **Fig S3** and **S4**). The PC2, representing 19.4% of the total variance, was associated with metabolites in cluster 1 including glycine that were depleted in all treatment combinations except in the controls and in the ineffective partnership between *Pbt* and Malibu (**Fig 3b2** Cluster 1). Oxoproline and some other metabolites shown in cluster 3 were intrinsically abundant in the shoots of Coronado.

Paraburkholderia's impact on Broccoli primary metabolism is associated with soluble sugars

As sugars are the primary drivers of plant growth, we looked into their temporal dynamics, particularly related to sugar generation and utilization in the shoots of the two Broccoli cultivars with or without the influence of the *Paraburkholderia* species. The fold change in sugar level between *Paraburkholderia* treated and control plants at 6dpi was used as a measure of sugar generation. While the temporal fold change in sugar level of treated plants from 6 to 11 dpi was used as a measure of sugar utilization. In control plants, sugars showed no significant change between the two Broccoli cultivars at 6 dpi (supplementary **Fig S3**). In contrast, treatment with the *Paraburkholderia* species showed unprecedented impact on the sugar generation in shoots of both Broccoli cultivars resulting in significant increases in the level of fructose and its derivatives, glucose, sorbose, galactose and galactopyranose at 6 dpi. Moreover, the magnitude of sugar generation showed remarkable difference between the *Paraburkholderia* species-Broccoli cultivar combinations (**Fig 3c1**). *Pbg* showed the highest sugar generation when compared to *Pbh* and *Pbt* and its sugar generation ability was significantly higher in Malibu cultivar. The ineffective partnership between *Pbt* and Malibu had the least significant impact on sugar generation. Similarly, the sugar utilization also showed noticeable differences among the *Paraburkholderia* species-Broccoli cultivar

combinations. In Coronado, *Pbg* inoculation led to greater sugar utilization when compared to cultivar Malibu. The ineffective partnership between *Pbt* and Malibu showed reduced sugar utilization when compared to the effective partnership of *Pbt* with Coronado (**Fig 3c2**).

Effects of Paraburkholderia on shoot secondary metabolism

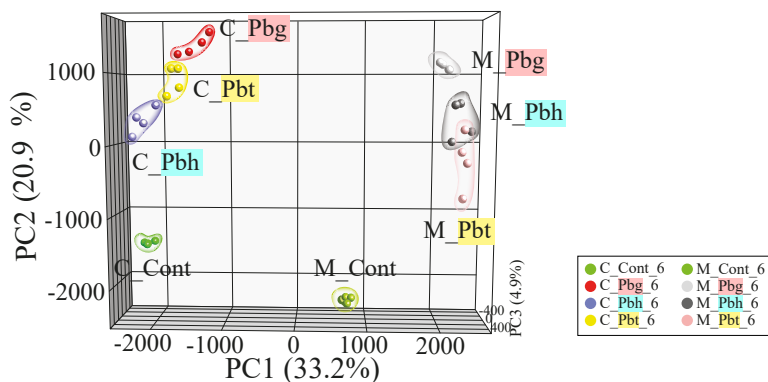
From the total of 1868 metabolites detected in positive or negative ionization mode, 1386 metabolites were significantly different between at least two treatments. PCA of the metabolites at 6 dpi demonstrated distinct clustering of the samples based on the *Paraburkholderia* species-Broccoli cultivar combination (**Fig 4a1**). The first PC explained 33.2% of the total variation and was associated with metabolites that were intrinsically abundant in one of the two Broccoli cultivars (Clusters **3**, **5** and **12**). Treatment of the two Broccoli cultivars with the *Paraburkholderia* species also widened the variation in the level of the metabolites that were intrinsically different between the two Broccoli cultivars. Metabolites that were intrinsically abundant in Coronado included aliphatic glucosinolates such as 2-methylbutyl glucosinolate and glucoiberberin as well as the aromatic glucosinolates glucotropaeolin and gluconasturtiin. The levels of aliphatic glucosinolates 2-methylbutyl glucosinolate and glucoiberberin were 147 and 209 times higher in Coronado when compared to Malibu, respectively (Cluster **3**). In Malibu, on the other hand, a number of metabolites from the phenylpropanoid pathway were intrinsically abundant (Clusters **5** and **12**). The second principal component (PC2) explained 20.9% of the total variance and was associated with metabolites that were reduced (**Fig 4b1** Clusters **2** and **4**) or induced (Clusters **7** and **11**) by the *Paraburkholderia* treatments. Inoculation of *Pbg* had the greatest impact on the shoot secondary metabolome profile of both Broccoli cultivars, whereas the ineffective partnership between *Pbt* and Malibu had less pronounced impact on the shoot metabolome. Metabolites in cluster **2**, comprising amino acids such as arginine, asparagine, tryptophan and N-acetylated glutamic acid/fucosamine, showed greater reduction in their abundance upon treatment with *Paraburkholderia* species. Cluster **4** encompassed metabolites that were more abundant in Malibu than Coronado and included ascorbic acid ethyl ester, N-acetyl-tryptophan, and terpenoids such as S-furanopetasitin and sonchuioside C. The metabolites in clusters **7** and **11** were induced by all the *Paraburkholderia* species and were dominated by phenylpropanoids. In Malibu, inoculation of *Pbg* led to greater accumulation of phenylpropanoids such as flavonoids glycosides (kaempferol-di/tri-(feruloyl/coumaroyl) glycosides and robinin), hydroxycinnamates (ferulic acid and its derivatives, caffeic acid derivatives such as chlorogenic acid) and an indole acetic acid derivative such as indole-3-acetic-acid-O-glucuronide when compared to the other two *Paraburkholderia* species. PC3 explained 4.9% of the total variance and was represented by *Pbg*-triggered (Clusters **8** and **10**) or *Pbt*-induced (Cluster **13**) metabolites in both Broccoli cultivars. *Pbg*-induced metabolites in cluster **8** consisted of the flavonoid kaempferol 3-sophorotrioside. Whereas *Pbt*-triggered metabolites in cluster **13** included the hydroxycinnamate 1,2-bis-O-sinapoyl-beta-D-glucoside and resveratrol-sulfolucoside, a stilbenoid.

Similarly, at 11dpi, inoculation with *Paraburkholderia* species led to substantial changes in the shoot metabolite profiles of the two Broccoli cultivars (**Fig 4a2** and **4b2**). In the PCA, the first three PCs explained 51.1% of the total variance. The first PC, explaining 29.1% of the total variance is associated with metabolites that accumulated or were reduced in response to *Paraburkholderia* and the change in these group of metabolites was more pronounced in Malibu cultivar (**Fig 4b2** Clusters **1, 2, 3, 4** and **5**: up, **10** and **11**: down). The induced metabolites in the above-mentioned clusters included flavonoids i.e. flavonol-di/tri-glycosides, kaempferol-di/tri-glycosides (feruloyl/caffeoyl/coumaroyl), robinin, medicarpin-O-glucoside-malonate, as well as hydroxycinnamates i.e. ferulic acid, caffeic acid and various derivatives of these metabolites. Furthermore, coumarins such as eupatoriochromene and mahaleboside and mevalonate, a precursor of mevalonate pathways that goes to terpenoid biosynthesis was also induced by the *Paraburkholderia* treatment. The reduced metabolites in both Broccoli cultivars included amino acids such as arginine, asparagine and acetyl/valyl conjugated amino acids i.e. valyl-methionine, and N-acetylglutamic acid (Cluster **10**). Meanwhile, metabolites in cluster **11** were also reduced by the *Paraburkholderia* treatment and these metabolites were intrinsically abundant in Coronado cultivar. Some of the metabolites in cluster **11** included sulfur-containing metabolites such as the aliphatic glucosinolates 2-methylbutyl glucosinolate and glucoiberberin, derivatives of sulfurous amino acids including leucyl-cysteine and methionyl-isoleucine, as well as precursor or breakdown products of glucosinolates, for instance, 6-methylthiohexanaloxime and 3-methylsulfinylpropyl isothiocyanate. The second PC (PC2) explained 23.8% of the total variance and was associated with metabolites that were intrinsically more abundant in cultivar Malibu (**Fig 4b2** Clusters **6, 7, 8** and **9**). Metabolites in clusters **6, 7, 8** and **9** showed significant depletion in all effective partnerships between the *Paraburkholderia* species and Broccoli cultivars. Tryptophan, a building block for indolic glucosinolate and the growth hormone indole-3-acetic acid, N-acetylated amino acid including N-acetyl phenylalanine/tryptophan, terpenoids i.e. S-furanopetasitin and sonchuioside C, and sulfuraphane an isothiocyanate are some of the metabolites in these cluster worth mentioning. PC3 explained 6.2% of the total variance and was associated with yet unknown metabolites that showed *Pbg* specific alteration in both Broccoli cultivars (Clusters **13**).

***Paraburkholderia* induces systemic resistance against the bacterial leaf pathogen *Xanthomonas campestris* in a cultivar-dependent manner**

As shown above, the two Broccoli cultivars exhibited inherent differences in their shoot chemistry (**Fig 4**). Furthermore, treatment of the plant roots with different *Paraburkholderia* species led to substantial alteration of the shoot metabolome including metabolome signatures specific to the individual combination of *Paraburkholderia* species and Broccoli cultivar (**Fig 4**). Based on this, we hypothesized that the inherent and induced differences in shoot chemistry between the two cultivars could contribute to a differential defense response against leaf pathogens. To address this hypothesis, treated and control plants of the two

a1



b1

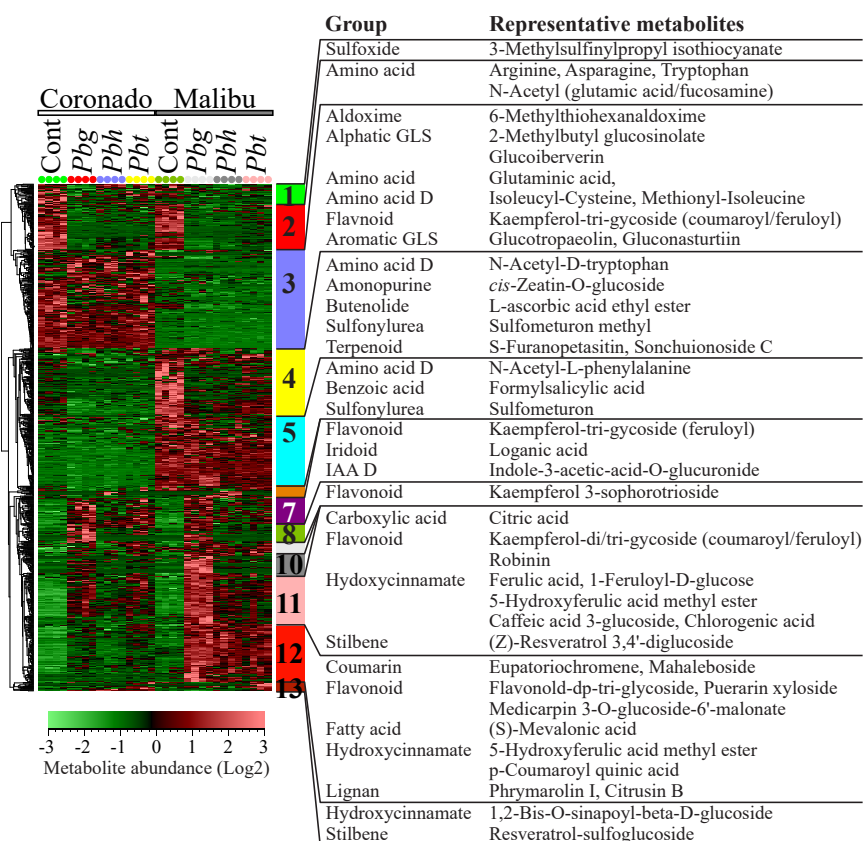
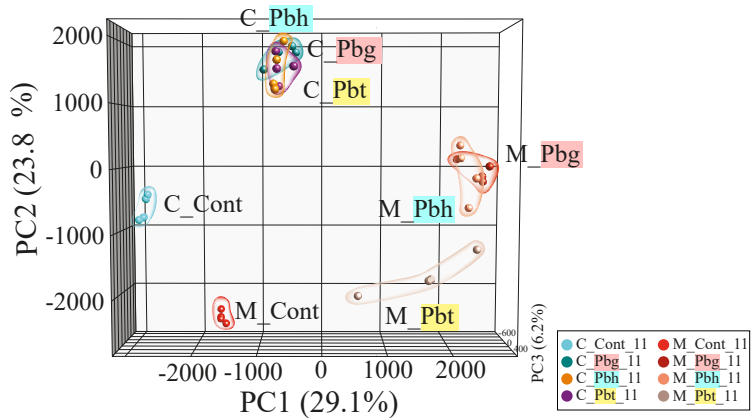


Fig 4. Rhizobacteria-mediated changes in the shoot secondary metabolites in Broccoli cultivars. (a) Principal component analysis (PCA) and (b) Hierarchical cluster analysis (HCA) based on differentially regulated metabolites of the samples at 6 dpi (1) and 11 dpi (2). In the HCA, metabolite clusters are indicated by different colors. Information on the representative metabolites of each clusters is given on the right side, if the metabolites are annotated. Broccoli cultivars (Cor: Coronado, Mal: Malibu), Cont.: non-rhizobacteria treated control, Pbg: *Paraburkholderia graminis*, Pbh: *P. hospita*, and Pbt: *P. terricola*. * GLS=glucosinolate, ** D=derivative.

a2



b2

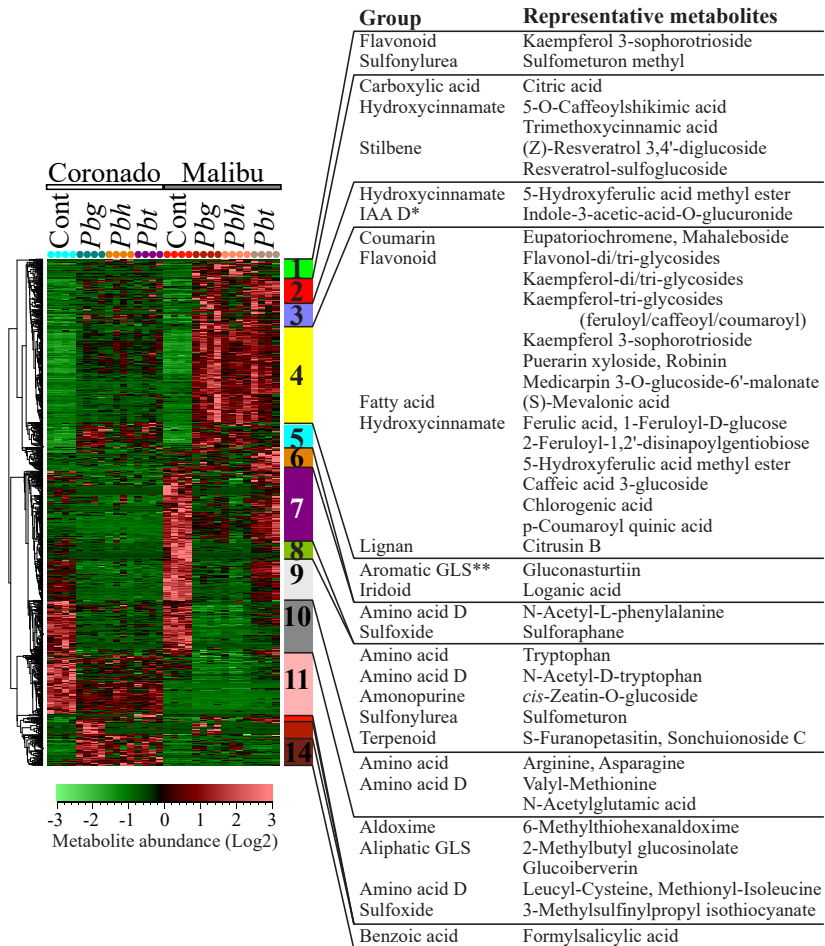


Fig 4. (Continued)

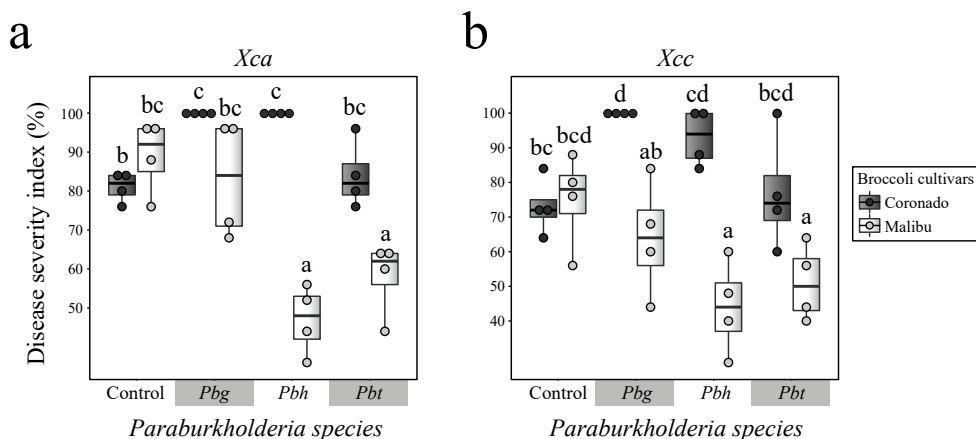


Fig 5. Impact of root-colonizing *Paraburkholderia* species on defense of Broccoli cultivars against two bacterial leaf pathogens. Disease severity index of two broccoli cultivars treated with either one of the three *Paraburkholderia* species and challenged with two bacterial leaf pathogens (a) *Xanthomonas campestris* pv. *armoraciae* P4216 (*Xca*) and (b) *Xanthomonas campestris* pv. *campestris* P4014 (*Xcc*). Broccoli cultivars (Cor: Coronado, Mal: Malibu), Control: non-treated control, *Pbg*: *Paraburkholderia graminis*, *Pbh*: *P. hospita*, and *Pbt*: *P. terricola*. Different letters show statistically significant differences between the treatments (Two-way ANOVA, Tukey's HSD *post hoc* test, $P < 0.05$).

cultivars were challenged with two bacterial leaf pathogens, i.e. *Xanthomonas campestris* pv. *armoraciae* P4216 (*Xca*) and *Xanthomonas campestris* pv. *campestris* P4014 (*Xcc*).

Regression analysis was employed to examine the interaction effect of two independent variables (*Paraburkholderia* species and Broccoli cultivars) on disease severity of the two bacterial pathogens using the “betareg” package in R. The *Paraburkholderia* species included three levels (*Pbg*, *Pbh* and *Pbt*) and the Broccoli cultivars consisted of two levels (Coronado and Malibu). There was a highly significant interaction effect of the *Paraburkholderia* species and Broccoli cultivars on disease severity for both *Xanthomonas* pathogens (Supplementary **Table S4**). No significant inherent variation in disease severity was observed between the two Broccoli cultivars when they were challenged with the two bacterial pathogens (**Fig 5**). However, treatment of the roots of the two Broccoli cultivars with the *Paraburkholderia* species led to a reduction or an enhancement of disease severity. For example, treatment with *Pbg* and *Pbh* enhanced disease severity in Coronado cultivar challenged by both bacterial pathogens, whereas *Pbh* and *Pbt* significantly reduced disease severity in cultivar Malibu challenged by each of the two bacterial pathogens (**Fig 5**).

Discussion

Our results showed that root-colonizing *Paraburkholderia* species altered shoot primary and secondary metabolism of Broccoli seedlings, promoted growth and induced systemic defense

against bacterial leaf pathogens. The magnitude of the alteration of these traits is dependent on the *Paraburkholderia* species and Broccoli cultivar combinations. The widely accepted “defense-growth tradeoff” concept asserts that activation of plant defense comes at the expense of plant growth due to resource limitations (Huot *et al.*, 2014). Here we showed that rhizobacteria treatment of plant roots promotes growth and at the same time primes the plant defense against biotic stress factors. Rhizobacteria defense priming is considered to have lower cost when compared to activation of direct defense (Martinez-Medina *et al.*, 2016). However, judging the cost of defense priming by only assessing some key physiological process such as seed production, number of flowers, pollen quality and number, and plant growth does not necessarily explain the energy and carbon costs associated with defense priming. Hence, to understand the underlying mechanisms by which rhizobacteria promote growth and prime the plant’s defense without compromising plant fitness, it requires a comprehensive investigation of the host metabolome network.

Root colonization by rhizobacteria is an important trait required for establishing beneficial effect on plant growth and health (Lugtenberg *et al.*, 2001; Compant *et al.*, 2010). In line with this, our study showed an association between root colonization ability of the *Paraburkholderia* species, their impact on the host metabolome and their ability to promote plant growth. For example, *Pbh* showed significantly reduced root colonization for cultivar Coronado at 6 dpi and its impact on both primary and secondary metabolism was the lowest when compared to *Pbg* and *Pbt* treated plants. Interestingly, at 11dpi, *Pbh* exhibited enhanced root colonization which coincided with an elevated impact on the shoot metabolome, comparable to that of plants treated with *Pbg* and *Pbt* (Fig 3 and 4 PCA). Similarly, *Pbt* showed significantly reduced root colonization for cultivar Malibu at both 6 and 11dpi with no significant growth promotion effect and the least impact on the shoot primary and secondary metabolism as compared to plants inoculated with *Pbg* and *Pbh*. The two Broccoli cultivars used in this study showed inherent differences in their shoot metabolome profile. Phenylpropanoids were more abundant in Malibu and glucosinolate and other sulfur-containing compounds showed higher abundance in Coronado. Assuming this variation in shoot chemistry may be reflected in differences in root chemistry, these intrinsic differences between the two cultivars might have influenced the root colonization ability of *Paraburkholderia* species and the effectiveness of the partnerships. Although the root exudate profile of the two Broccoli cultivars was not assessed in our study, exudate composition of plant species has a major impact on microbiome assembly and functions in the rhizosphere (Philippot *et al.*, 2013; Pérez-Jaramillo *et al.*, 2016; Hu *et al.*, 2018; Lundberg & Teixeira, 2018; Pérez-Jaramillo *et al.*, 2018; Stringlis, Ioannis A *et al.*, 2018; Huang *et al.*, 2019). Assessing the root exudate profile of the two broccoli cultivars in combination with bioassay-guided fractionation of the exudates will be instrumental to identify metabolite signatures that govern the differences in root colonization by the *Paraburkholderia* species and the effectiveness of their partnership with different Broccoli cultivars.

4

The *Paraburkholderia* species exerted a substantial impact on the host primary and secondary metabolism at both early and late stages of seedling growth. Their biggest impact on primary metabolism was reflected in soluble sugar generation and utilization and both parameters showed significant variation across the *Paraburkholderia* species - Broccoli cultivar combinations (**Fig 3c**). All combinations, except *Pbt*-Malibu, resulted in effective partnership, i.e. plant growth promotion. Effective partnerships showed higher soluble sugar generation at the early stage of seedling growth and high sugar utilization at the later stage of seedling growth, whereas the ineffective partnership between Malibu and *Pbt* showed reduced sugar generation and utilization. Soluble sugars are fuel for growth and for the biosynthesis of secondary metabolites involved in defense (Herrmann & Weaver, 1999; Hartmann & Trumbore, 2016). Moreover, soluble sugars such as galactose, glucose, sorbose, fructose, sucrose and xylose have been reported to be effective chemotaxis agents for bacteria (Adler *et al.*, 1973; Ordal *et al.*, 1979). Their increased production under effective partnership between plants and rhizobacteria could provide both the plants and rhizobacteria with fuel for energy production to sustain growth and secondary metabolite production. In general, low sugar concentration promotes ‘source’ activities such as photosynthesis, nutrient mobilization and export, while high sugar level enhances ‘sink’ activities such as growth and sugar storage (Rolland *et al.*, 2006). Hence, we postulate that the enhancement of the sugar levels is a key mechanism that determines the effectiveness of the partnership between rhizobacteria and plants. Furthermore, under effective partnership, there was significantly higher depletion (>11-fold) of PEP, a key substrate for the TCA cycle and the shikimate pathway (**Fig 6**), whereas PEP depletion was only about 2-fold under ineffective partnership. Furthermore, greater depletion of GABA under the effective partnership suggests catabolism of GABA to succinyl semialdehyde followed by its conversion to succinate to feed the greater demand of pyruvate in the TCA cycle. Key intermediates in the TCA cycle such as citric acid and malic acid showed increased abundance under effective partnership. In the TCA cycle, citrate is converted to malate and used in the mitochondria for energy production (Fernie *et al.*, 2004). Hence, these observations most likely meet the greater demand for carbon and energy occurring during enhanced growth and defense priming in the effective *Paraburkholderia*-Broccoli interactions.

For the soluble sugars, *Paraburkholderia* species showed their biggest impact on fructose abundance. *Pbg*-Malibu interaction showed the highest root colonization and had the highest impact on shoot fructose level (~>280 folds). In contrast, *Pbt*-Malibu and *Pbh*-Coronado interactions showed the lowest root colonization levels and had the lowest impact on shoot fructose generation at the early stages of seedling growth. Interestingly, the biggest impact on shoot fructose abundance by *Pbg* also showed the biggest impact on secondary metabolism in general and phenolic compounds accumulation in particular when compared to *Pbh* and *Pbt* at 6 dpi (**Fig 6**). This suggests that the effects of elevated levels of soluble sugars are not only limited to plant growth but also extend to secondary metabolites biosynthesis. For example, fructose is the primary substrates for fructose-6-phosphate, a key substrate for the

biosynthesis of both PEP and erythros-4-phosphate (**Fig 6**). These two intermediates are channeled to the shikimate pathway that bridges carbohydrate metabolism to biosynthesis of aromatic primary and secondary metabolites (Herrmann & Weaver, 1999). The shikimate pathway provides all the important precursors for the biosynthesis of phenylpropanoids including hydroxycinnamates, flavonoids, stilbenoids, coumarins and lignins that showed significant accumulation in plants treated with *Paraburkholderia* species (**Fig 4b** and **6**). A study on the *pho3* mutant of Arabidopsis that accumulates soluble sugars to high levels, showed large increases in the expression of transcriptional factors and enzymes involved in anthocyanin biosynthesis (Lloyd & Zakhleniuk, 2004). Another study also showed greater accumulation of fructose (~10 fold) and flavonoids in quinoa cotyledons in response to UV-B radiation (Hilal *et al.*, 2004). Considering our results and the aforementioned findings by other studies, we postulate that one of the key mechanisms by which rhizobacteria modulate host secondary metabolism is by soluble sugar generation.

In addition to enhancement of key precursors for growth and secondary metabolite biosynthesis, treatment of *Paraburkholderia* also induced metabolite remobilization. The metabolite remobilization involved both suppression of resource competing metabolite pathways such as amino acids and rechanneling of existing primary metabolite-derivatives and other secondary metabolites to other metabolite pathways. For example, aromatic glucosinolate, amino acids and their derivatives, some terpenoids showed more depletion in effective partnerships (**Fig 6** and **Fig 4b2**). Hence, remobilization of the existing metabolites towards targeted metabolite pathways could be an additional strategy used by rhizobacteria to reduce the cost of *de novo* biosynthesis of metabolites.

Our results also showed that rhizobacteria-mediated reorganization of the host metabolome landscape not only affects plant growth but also the defense response of Broccoli cultivars to bacterial leaf pathogens. In general, inoculation of the *Paraburkholderia* species showed greater suppression of pathogen proliferation in cultivar Malibu that intrinsically has more phenolic compounds (**Fig 5**). The phenylpropanoid pathway appears to be the central target by the *Paraburkholderia* species and was altered to a greater extent in Malibu than in Coronado (**Fig 6**). All metabolite classes belonging to this pathway including flavonoids, hydroxycinnamates, stilbenoids, coumarins and lignins showed substantial accumulation upon treatments with the *Paraburkholderia* species (**Fig 6**). These metabolites were reported to have direct antimicrobial effects and/or act as a physical barrier against pathogenic microorganisms (Dixon *et al.*, 2002; Cvikrova *et al.*, 2006). Hydroxycinnamic acids and flavonoid were shown to negatively affect the disease symptom development in Chinese cabbage challenged by *Xanthomonas campestris* pv. *campestris* (*Xcc*) (Islam *et al.*, 2018). Of all the *Paraburkholderia* species-Broccoli cultivars combinations, treatment of roots of cultivar Coronado with *Pbg* resulted in higher disease severity (**Fig 5**). However, we could not find a specific metabolic signature that corresponds to the increased pathogen susceptibility of Coronado treated with *Pbg*.

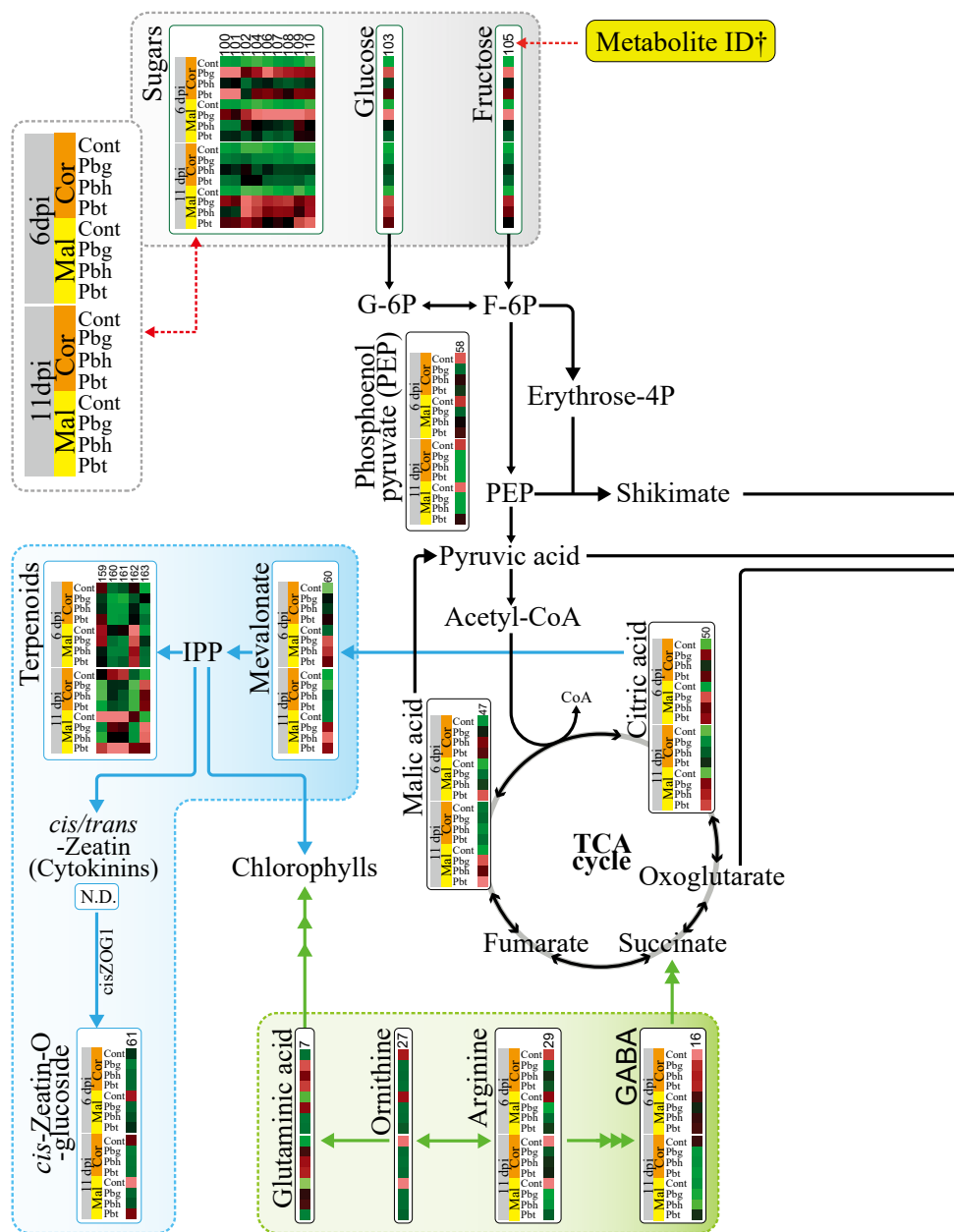
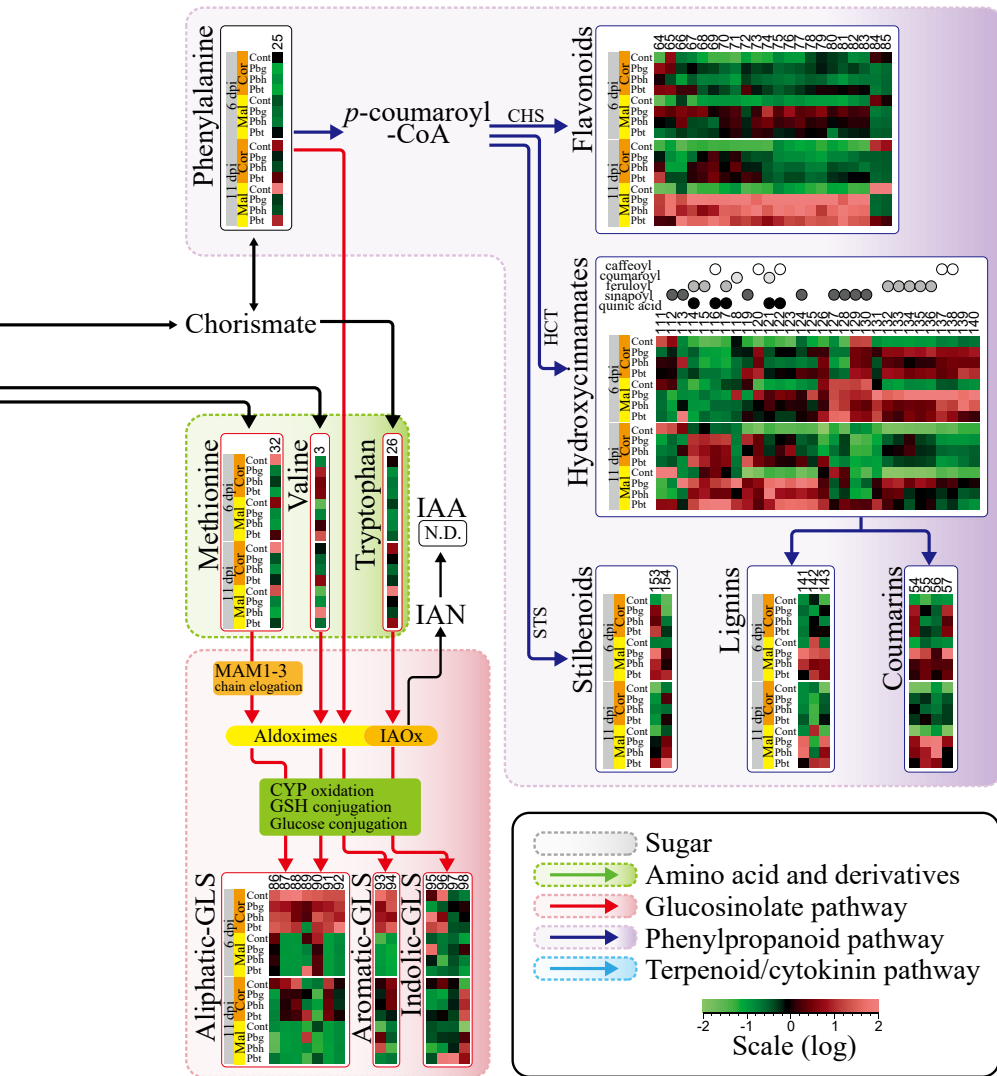


Fig 6. Alteration of core primary and secondary metabolite pathways by *Paraburkholderia* species in Broccoli. The metabolite pathways are organized as modules inside different colored boxes and the abundance of the significantly altered metabolites is represented by the heat map where each cells representing the abundance of a metabolite of a sample for *Paraburkholderia* species-Broccoli cultivar and time combinations. The metabolite ID corresponding to each metabolites is indicated at the top of the heat map and detailed information on the identity of the individual metabolites is provided in the supplementary excel **Table S9**. G-6P (Glucose 6-phosphate), F-6P (Fructose 6-phosphate), CHS



(Chalcone synthase), cisZOG1 (Cis-zeatin O-glucosyltransferase 1), CYP (Cytochrome P450), GABA (γ -aminobutyric acid), GLS (Glucosinolates), GSH (Glutathione), HCT (hydroxycinnamoyl-CoA shikimate/quinate hydroxy-cinnamoyl transferase), IAA (indole-3-acetic acid), IAN (indole-3-acetonitrile), IAOx (indole-3-acetaldoxime), IPP (isopentenyl pyrophosphate), MAM (methylthioalkylmalate synthase), and STS (stilbene synthase). Broccoli cultivars (Cor: Coronado, Mal: Malibu), Cont.: non-rhizobacteria treated control, Pbg: *Paraburkholderia graminis*, Pbh: *P. hospita*, and Pbt: *P. terricola*. Multiple-headed arrows indicate hidden intermediate processes in the pathways.

4

Defense priming is not a low-cost defensive measure as postulated but could cost substantial amounts of energy and carbon resources. This is shown by the massive accumulation of phenylpropanoids and other defensive compounds in plants primed by *Paraburkholderia* species even before the plants were challenged with the bacterial leaf pathogens. The integrated primary and secondary metabolome profiling of primed plants suggests that rhizobacteria could avert the negative impact of defense priming on the host fitness by generating massive amount of soluble sugars and remobilizing other metabolites to accommodate for the high energy and carbon skeleton demand associated with growth and defense priming. This could indicate that defense costs can be regulated if resources are not limiting and aligns with studies that showed the inevitability of defense-growth trade-off occurs primarily under resource-limiting conditions (Bergelson & Purrington, 1996; van Dam & Baldwin, 1998).

The magnitude of the impact of the rhizobacteria on plant growth, metabolism and defense priming showed an association with the level of root colonization by the rhizobacteria. On the other hand, the plant genotype and its intrinsic chemical composition could affect the ability of the rhizobacteria to colonize the host root and could determine the impact rhizobacteria have on different phenotypic traits of the host. Hence, breeding of plant for different traits should consider its impact on the host chemistry and its associated effect on the recruitment of beneficial microbes for the plant functioning. Furthermore, investigating the underlying mechanism of rhizobacteria-mediated generation of soluble sugars in plants could be instrumental for breeding programs that aim to produce high yielding and stress-resilient crops. Hence, further studies on beneficial bacterial traits involved in the modulation of the host metabolism could provide information on the underlying mechanisms of rhizobacteria-mediated alteration of host metabolism, growth and defense priming.

Acknowledgements

Seeds of two Broccoli cultivars (*Brassica olearacea* var. *italic*), Coronado and Malibu, were kindly provided by Bejo seed company (Warmenhuizen, The Netherlands). We are grateful to Bert Schipper and Henriëtte Vaneekelen for their help with LC MS analysis and pre-processing of metabolomics data.

Supplementary materials

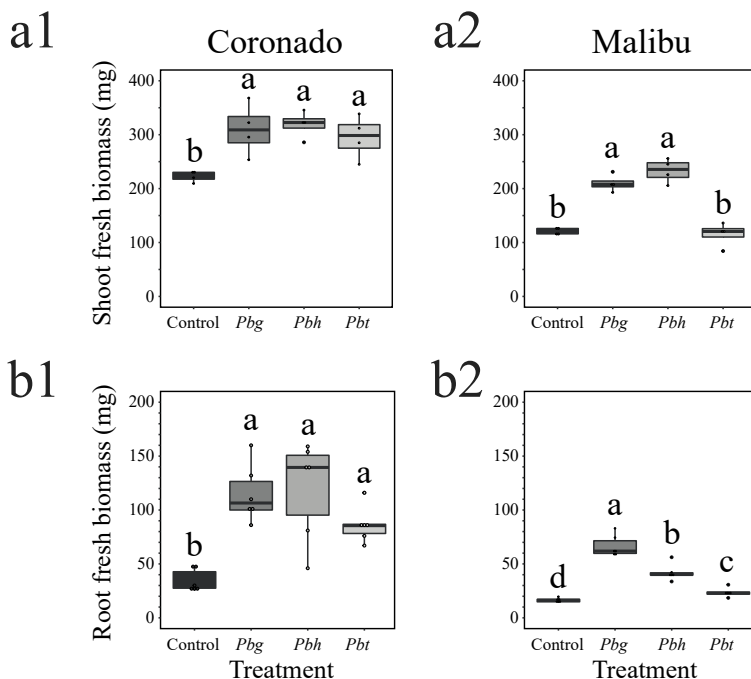


Fig S1. Absolute changes in shoot (a) and root (b) biomass of Broccoli cultivars Coronado (1) and Malibu (2) at 11 dpi with *Paraburkholderia* species. *Pbg*: *Paraburkholderia graminis*, *Pbh*: *P. hospita*, and *Pbt*: *P. terricola*. Different letters show significant statistical difference between the treatments (One-way ANOVA, Tukey's HSD *post hoc* test, $P < 0.05$).

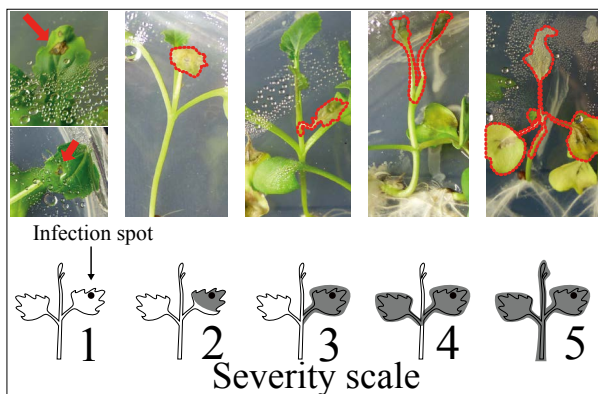


Fig S2. Disease severity scale. For the severity (c), each Broccoli seedlings from four biological replicates were individually scored ($n = 20$). Disease severity was scored by determining the migration of the lesion from the inoculation spot to the other parts of the shoot following an ordinal scale from 1- 5, where 1 = no necrosis or migration, 2 = full infection of the treated leaf, 3 = migration to the leafstalk of the treated leaf, 4 = infection of the neighboring leaf, and 5 = infection of the entire seedling.

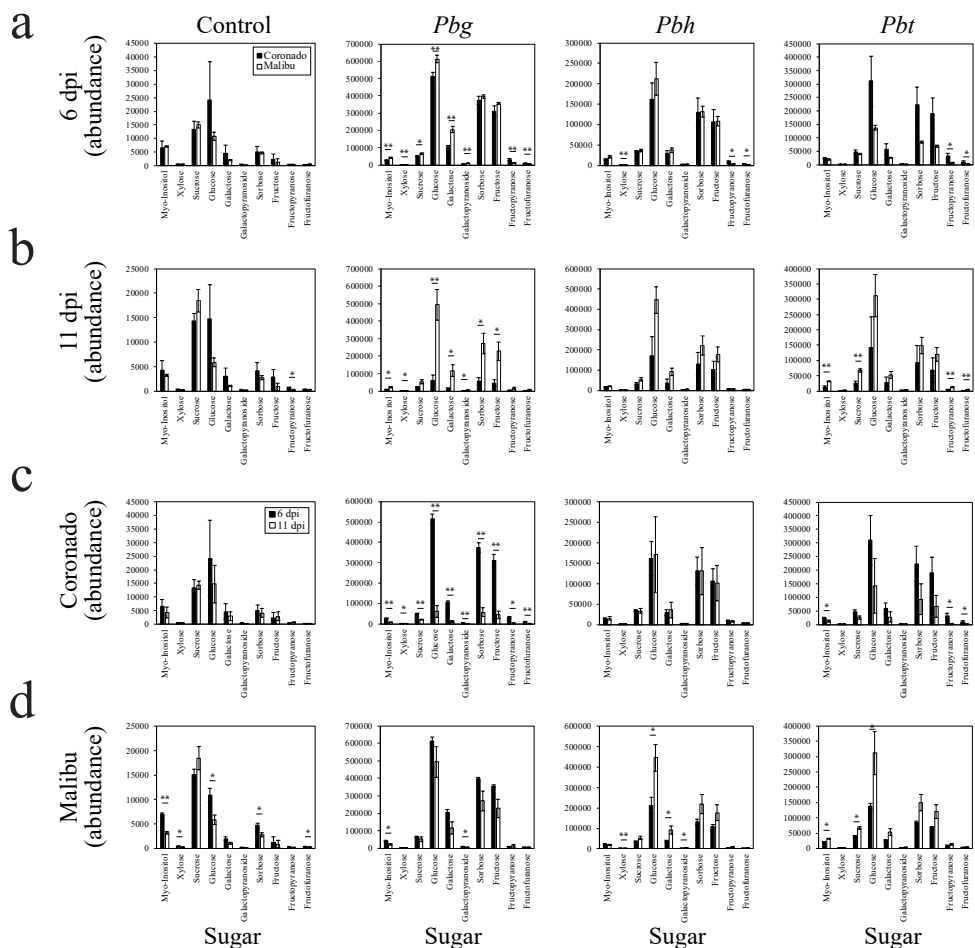


Fig S3. Absolute abundance of soluble sugars in two Broccoli cultivars upon *Paraburkholderia* inoculation at two time points (6 and 11 dpi). Comparative analysis of the of abundance of soluble sugars between the two cultivars at 6 dpi (**a**) and at 11 dpi (**b**). Comparative analysis of the abundance of soluble sugars at two time points in Coronado (**c**) and Malibu (**d**) cultivars. *Pbg*: *Paraburkholderia graminis*, *Pbh*: *P. hospita*, and *Pbt*: *P. terricola*. Asterisks denote significant statistical differences between Broccoli cultivars, Coronado and Malibu (two tailed Student's t test): * $P < 0.05$; ** $P < 0.01$.

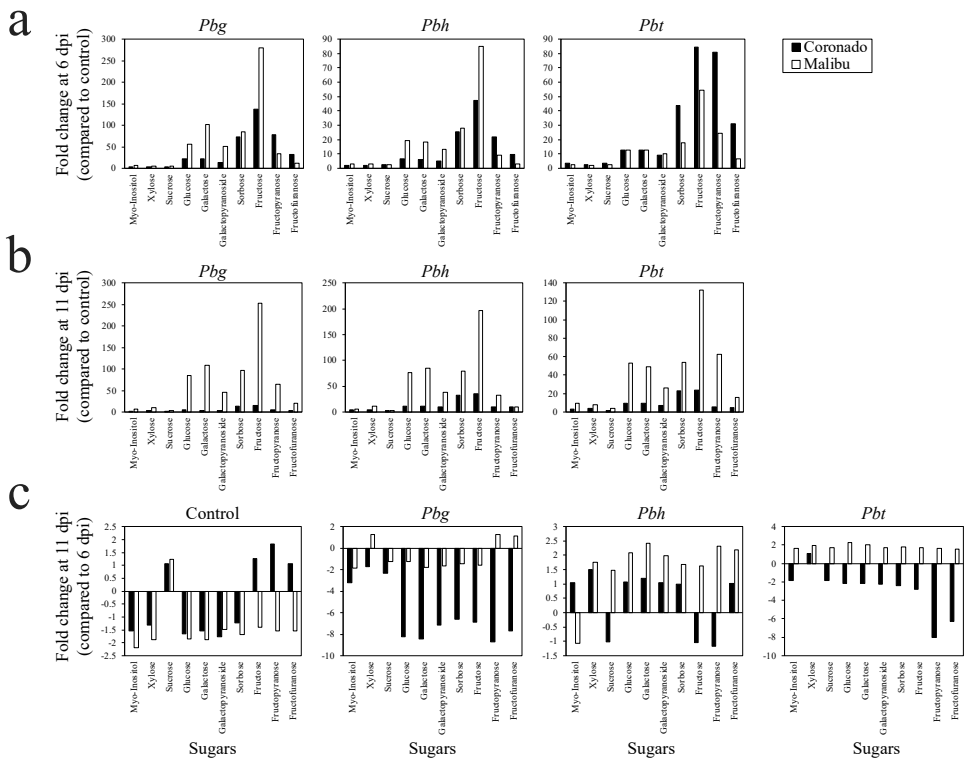


Fig S4. *Paraburkholderia* species-mediated changes in shoot soluble sugar abundance in two Broccoli cultivars, Coronado and Malibu, at 6 dpi (a), 11 dpi (b), and relative fold change between the two time points (c). In (a) and (b), fold change was calculated by dividing the abundance of each soluble sugars in treated plants to that of the non-treated control. *Pbg*: *Paraburkholderia graminis*, *Pbh*: *P. hospita*, and *Pbt*: *P. terricola*.

Table S1. Analysis of variance ANOVA (type II) of percent changes in shoot and root biomass in two Broccoli cultivars inoculated with three *Paraburkholderia* genera at 11 dpi.

Sample	Factor	Sum Sq	Df	F value	Pr(>F)	
Shoot fresh biomass relative change	Broccoli cultivars	1425	1	4.882	0.040333	*
	Bacteria species	12949	2	22.182	1.39E-05	***
	Broccoli cultivars: Bacteria species	8561	2	14.665	0.000166	***
	Residuals	5254	18			
Root fresh biomass relative change	Broccoli cultivars	1210.18	2	19.711	3.42E-06	***
	Bacteria species	142.42	1	4.6394	0.039404	*
	Broccoli cultivars: Bacteria species	400.55	2	6.5241	0.004441	**
	Residuals	920.94	30			

Significance codes: *** 0, ** 0.001, * 0.01.

Table S2. Population density of three *Paraburkholderia* species on roots of two Broccoli cultivars. *Pbg*: *Paraburkholderia graminis*, *Pbh*: *P. hospita*, and *Pbt*: *P. terricola*.

Broccoli cultivar	Rhizobacteria	Population density (Cfu/mg roots)	
		6 dpi	11 dpi
Coronado	<i>Paraburkholderia graminis</i>	2.05 ± 0.11 x 10 ⁸	8.10 ± 0.28 x 10 ⁷
	<i>P. hospita</i>	1.18 ± 0.09 x 10 ⁶	2.06 ± 0.08 x 10 ⁷
	<i>P. terricola</i>	1.58 ± 0.03 x 10 ⁷	1.95 ± 0.04 x 10 ⁷
Malibu	<i>P. graminis</i>	1.00 ± 0.05 x 10 ⁸	1.02 ± 0.07 x 10 ⁸
	<i>P. hospita</i>	1.40 ± 0.15 x 10 ⁷	1.53 ± 0.06 x 10 ⁷
	<i>P. terricola</i>	1.72 ± 0.16 x 10 ⁶	7.02 ± 0.35 x 10 ⁵

Cfu: Colony forming unit

*Values represent the average of 3 replicates ± SE of three replicates

Table S3. Analysis of variance ANOVA (type II) of root colonization of three *Paraburkholderia* species in two Broccoli cultivars at two time points (6 dpi, 11 dpi). Data was log transformed using the package MASS in R.

Factor	Sum Sq	Df	F value	Pr(>F)	
Day post inoculation	0.0887	1	41.745	1.11E-06	***
Broccoli cultivar	0.7069	1	332.569	1.44E-15	***
Bacteria species	13.4135	2	3155.343	< 2.2e-16	***
Day post inoculation: Broccoli cultivar	0.4061	1	191.066	6.35E-13	***
Day post inoculation: Bacteria species	1.3366	2	314.421	< 2.2e-16	***
Broccoli cultivar: Bacteria species	4.353	2	1023.972	< 2.2e-16	***
Day post inoculation: Broccoli cultivar: Bacteria species	0.9733	2	228.966	2.33E-16	***
Residuals	0.051	24			

Signif. codes: 0 =***, 0.001 = **, 0.01 = *

Table S4. Beta regression analysis of disease severity in two Broccoli cultivars (Coronado and Malibu) primed with *Paraburkholderia* species and treated with *Xanthomonas*, a Broccoli leaf pathogen. Different *Paraburkholderia* species were used to induced systemic resistance. *Xca*: *Xanthomonas campestris* pv. *Armoraciae* P4216 and *Xcc*: *X. campestris* pv. *Campestris* P4014.

Pathovar	model term	df1	df2	F.ratio	p.value
<i>Xca</i>	Rhizobacteria	3	Inf	11.74	<.0001
	Broccoli cultivar	1	Inf	64.893	<.0001
	Rhizobacteria:Broccoli cultivar	3	Inf	20.627	<.0001
<i>Xcc</i>	Rhizobacteria	3	Inf	3.811	0.0096
	Broccoli cultivar	1	Inf	49.535	<.0001
	Rhizobacteria:Broccoli cultivar	3	Inf	7.604	<.0001

Table S5. *Paraburkholderia* species-mediated changes in shoot polar primary metabolites (GC-MS) in two Broccoli cultivars (Coronado and Malibu) at 6 dpi. The tabulated data corresponds to the hierarchical cluster analysis (HCA) shown in **Fig 3b1** of the manuscript. The fold change corresponding to each metabolites was calculated by dividing the abundance of each metabolites in *Paraburkholderia* treated plants to the non-treated control. *Pbg*: *Paraburkholderia graminis*, *Pbh*: *P. hospita*, and *Pbt*: *P. terricola*.

Cluster Number	Mapping Number	RT(m)	Mass	RI		Annotation	Fold change					
				Observed	in DB		Coronado			Malibu		
							<i>Pbg</i>	<i>Pbh</i>	<i>Pbt</i>	<i>Pbg</i>	<i>Pbh</i>	<i>Pbt</i>
1		16.6	73	1848	1846	4-(2-Aminoethyl)-2-methoxyphenol, 3TMS derivative	-8.54	-6.92	-1.48	-8.19	-5.17	-5.01
2		13.0	55	1529	1529	Hexamethylene diacrylate	-1.58	-1.8	-1	-5.82	-5.37	-3.47
2	18	12.8	73	1520	1522	L-5-Oxoproline	-1.4	-1.38	-1.43	-3.07	-2.81	-2.28
2	16	12.9	73	1523	1525	GABA	-1.23	-1.26	-1.25	-1.74	-1.64	0.67
4	10	9.8	73	1286	1286	Isoleucine	-2.16	-2.82	-3.21	0.49	0.25	0.43
4		11.2	174	1387	1386	Ethyl 2,4-Dimethylbenzoate	-1.16	-1.21	-1.7	0.4	-2.84	0.69
4	12	15.7	73	1767	1768	Glutamine	-1.36	-1.32	-2.65	-3.67	-3.38	-2.24
5	25	14.1	73	1623	1624	L-Phenylalanine	-1.94	-1.6	-1.93	-1.31	-1.47	1.01
5		8.5	73	1192		Methyl 7-Trimethylsilylheptanoate	-5.11	-2.09	-2.81	-3.99	-2.64	-2.32
5	31	17.2	73	1910	1912	Lysine	-3.61	-2.87	-4.21	-2.54	-2.89	-2.23
5		13.5	73	1573		Trimethyl[(2E/Z)-6-(2-thienyl)-2,6-heptadienyl]silane	-2.52	-1.94	-3.12	-2.53	-1.95	-1.64
5		12.0	73	1453	1452	N,N-Diethyl 6-oxoheptamide	-16.07	-4.09	-16.43	-18.08	-10.83	-10.08
5	32	12.8	176	1514	1515	Methionine	-2.85	-2.19	-3.51	-3.09	-2.9	-1.85
5		13.7	73	1591	1595	Diethyl (2R/S,3R)-2-Allyl-3-(trimethylsiloxy)succinate	-3.45	-2.42	-3.28	-4.1	-3.7	-2.73
5		14.6	73	1669	1673	7,8-Dehydro-8-deoxocurcumen-11-ol	-3.05	-2.05	-3.23	-3.1	-2.56	-1.96
5	58	9.5	73	1263	1263	Phosphoenolpyruvate	-3.81	-2.05	-2.63	-3.48	-2.32	-1.76
6	27	16.1	73	1805		DL-Ornithine	-12.52	-10.61	-13.78	-11.85	-8.33	-6.05
7	47	12.3	73	1479	1480	Malic acid	1.31	1.57	1.48	1.12	1.48	1.71
7	22	10.0	73	1299	1300	Glycine	-1.08	1.23	1.03	0.77	1.01	1.28
7	6	13.9	73	1611	1612	Glutamic acid	1.28	1.14	1.13	1.24	-1.35	0.99
8	4	11.6	73	1420	1420	L-Aspartic acid	2.3	1.67	4.18	2.96	2.67	1.97
8	146	17.9	73	1977	1981	Mannonic acid, lactone	1.96	-1.24	4.08	1.59	0.87	0.62
8		9.4	73	1259	1260	TMS 4-DI-TMS-AMINOBUTYRATE	3.22	1.55	1.7	1.68	1.86	1.76
8	8	15.3	73	1729	1731	Putrescine	1.44	1.09	1.42	1.18	1.02	0.95
9	45	16.5	73	1839	1863	Ascorbic acid	1.5	1.34	1.46	1.85	1.49	1.71
9		16.9	191	1877	1877	2-Amino-3-cyano-4-(2'-furyl)-4-thioxobut-2-ene	28.8	5.29	24.23	20.2	2.46	4.7
9	101	16.1	73	1801	1802	D-(-)-Fructopyranose (isomer 2)	78.58	22.07	80.8	26.95	10.85	15.98
9	100	16.0	73	1795	1792	D-(-)-Fructofuranose (isomer 1)	32.09	9.51	31.1	15.76	5.46	7.45
9	102	14.3	73	1640	1634	Xylose	3.71	2.08	2.64	4.77	2.75	2.96
9	105	16.7	73	1863	1865	Fructose	138.02	47.19	84.47	157.82	40.86	37.71
9	109	18.8	73	2074	2077	Myo-Inositol	4.06	2.18	3.69	6.29	2.58	3.45
9	110	23.3	73	2606	2611	Sucrose	3.8	2.52	3.57	4.89	2.76	2.86
9	106	16.6	73	1854	1854	Sorbose	73.61	25.66	43.78	77.87	21.94	20.4
9	107	18.2	73	2010	2010	D-Galactopyranoside	14.23	5.01	9.38	23.53	5.31	5.29
9	108	17.1	73	1899	1898	d-Galactose, 2,3,4,5,6-pentakis-O-(trimethylsilyl)-, o-methoxyyme, (1E)-	22.64	6.32	12.58	44.36	6.79	6.93
9	103	16.9	73	1879	1881	Glucose	21.19	6.66	12.81	25.26	6.97	7.46

Table S6. *Paraburkholderia* species-mediated changes in shoot polar primary metabolites (GC-MS) in two Broccoli cultivars (Coronado and Malibu) at 11 dpi. The tabulated data corresponds to the hierarchical cluster analysis (HCA) shown in **Fig 3b2** of the manuscript. The fold change corresponding to each metabolites was calculated by dividing the abundance of each metabolites in *Paraburkholderia* treated plants to the non-treated control. *Pbg*: *Paraburkholderia graminis*, *Pbh*: *P. hospita*, and *Pbt*: *P. terricola*.

Cluster Number	Mapping Number	RT(m)	Mass	RI		Annotation	Fold change					
				Observed	in DB		Coronado			Malibu		
							<i>Pbg</i>	<i>Pbh</i>	<i>Pbt</i>	<i>Pbg</i>	<i>Pbh</i>	<i>Pbt</i>
1	22	10.0	73	1299	1300	Glycine	-1.16	-1.84	-1.29	-2.4	-1.22	-1.14
2	32	12.8	176	1514	1515	Methionine	-2.37	-3.18	-2.1	-2.59	-3.39	-1.95
2		13.5	73	1573		Trimethyl[(2E/Z)-6-(2-thienyl)-2,6-heptadienyl]silane	-2.22	-2.21	-2.41	-2.06	-2.12	-1.4
2		14.6	73	1669	1673	7,8-Dehydro-8-deoxocurcumen-11-ol	-2.27	-2.16	-2.36	-2.31	-2.49	-1.7
2		12.0	73	1453	1452	N,N-Diethyl 6-oxoheptamide	-11.7	-4.59	-3.09	-11.19	-10.7	-4.25
2		13.7	73	1591	1595	Diethyl (2R/S,3R)-2-Allyl-3-(trimethylsilyloxy)succinate	-2.14	-2.12	-2.35	-2.7	-2.95	-2.89
2	25	14.1	73	1623	1624	L-Phenylalanine	-1.05	-1.17	-0.83	-2.72	-2.86	-1.63
2	58	9.5	73	1263	1263	Phosphoenolpyruvate	-14.18	-11.91	-12.75	-11.43	-11.3	-2.13
2	31	17.2	73	1910	1912	Lysine	-2.71	-2.55	-2.75	-3.47	-3.4	-2.92
2	27	16.1	73	1805		DL-Ornithine	-10.86	-14.9	-10.33	-23.84	-22.03	-13.68
2		16.6	73	1848	1846	4-(2-Aminoethyl)-2-methoxyphenol, 3TMS derivative	-6.71	-10.66	-10.6	-11.9	-13.78	-8.23
2		8.5	73	1192		Methyl 7-Trimethylsilylheptanoate	-7.85	-3.95	-3.55	-2.19	-3.16	-1.29
2	16	12.9	73	1523	1525	GABA	-2.38	-2.31	-2.44	-1.13	-1.27	1.31
3		13.0	55	1529	1529	Hexamethylene diacrylate	-9.3	-13.75	-12.34	1.09	1.07	1.44
3	18	12.8	73	1520	1522	L-5-Oxoproline	-2.49	-2.15	-2.3	1.03	-1.11	1.01
5	8	15.3	73	1729	1731	Putrescine	1.42	1.36	1.32	4.01	3.62	2.83
5		9.4	73	1259	1260	TMS 4-DI-TMS-AMINO BUTYRATE	3.61	2.89	3.65	2.61	2.84	2.16
5	4	11.6	73	1420	1420	L-Aspartic acid, 2TMS derivative	1.74	2.07	1.77	3.03	4.77	3.4
5	110	23.3	73	2606	2611	Sucrose	1.63	2.47	1.91	2.84	2.89	3.65
5	102	14.3	73	1640	1634	Xylose	2.13	3.11	2.88	10.9	10.76	7.98
5	105	16.7	73	1863	1865	Fructose	20.05	45.02	30.13	252.76	196.15	132.07
5	109	18.8	73	2074	2077	Myo-Inositol	1.26	2.26	2.03	7.05	6.12	9.87
5	106	16.6	73	1854	1854	Sorbose	11.13	25.71	18.28	97.3	79.09	53.56
5	107	18.2	73	2010	2010	D-Galactopyranoside, methyl 2,3,4-tris-O-(trimethylsilyl)-, acetate	1.99	5.2	4.14	45.56	38.49	25.88
5	103	16.9	73	1879	1881	Glucose	2.57	7.06	5.83	84.07	75.88	53.04
5	108	17.1	73	1899	1898	d-Galactose, 2,3,4,5,6-pentakis-O-(trimethylsilyl)-, o-methoxy, (1E)-	2.68	7.65	5.92	107.78	84.51	48.95
5	45	16.5	73	1839	1863	Ascorbic acid	1.19	1.39	0.91	2.13	2.33	2.55
6	6	13.9	73	1611	1612	Glutamic acid	1.05	1.12	1.22	1.66	1.57	1.69
6	5	12.7	73	1511	1512	ASPARTIC ACID-TRITMS	-1.47	1.1	1.04	2.22	1.78	2.46
6	101	16.1	73	1801	1802	D(-)-Fructopyranose (isomer 2)	9.02	18.82	10.12	64.34	32.8	62.32
6	100	16.0	73	1795	1792	D(-)-Fructofuranose (isomer 1)	4.18	9.7	4.95	20.31	10.47	15.98

Table S7. *Paraburkholderia* species-mediated changes in shoot semi-polar secondary metabolites (LC-MS) in two Broccoli cultivars (Coronado and Malibu) at 6 dpi. The tabulated data corresponds to the hierarchical cluster analysis (HCA) shown in **Fig 4b1** of the manuscript. The fold change corresponding to each metabolites was calculated by dividing the abundance of each metabolites in Paraburkholderia treated plants to the non-treated control. *Pbg*: *Paraburkholderia graminis*, *Pbh*: *P. hospita*, and *Pbt*: *P. terricola*.

Cluster number	Mapping number	RT (m)	m/z	Mass (D)	Compound	Formula	ppm to DB	Classification	data base	Fold change					
										Coronado			Malibu		
										<i>Pbg</i>	<i>Pbh</i>	<i>Pbt</i>	<i>Pbg</i>	<i>Pbh</i>	<i>Pbt</i>
2	157	17.46	[M+H] ⁺	16401952	3-Methylsulfinylpropyl isothiocyanate	C3H9NO2	-1.64	Sulfoxide	HMDB	-3.4	-2.3	-3.0	-1.2	-1.4	-1.4
2	3.00	[M+H] ⁺	144054932	1-Pyrroline-2-carboxylic acid	C5H7NO2	-0.39	Pyroline	HMDB	-1063.2	-146.0	-16.1	-1425.4	-1410.1	-23.4	-23.4
2	111	20.19	[M+H] ⁺	56176819	4-Demethylsimmondsin 2'-(E)-ferulate	C25H31NO12	-0.99	Coumaric acid	HMDB	-1.8	-1.4	-1.5	-1.4	-1.4	-1.4
2	29	1.63	[M+H] ⁺	17511820	Arginine	C6H14N4O2	-0.89	Amino acid	KEGG	-3.3	-2.0	-2.4	-4.6	-2.2	-1.7
2	30	1.87	[M+H] ⁺	17310456	Arginine	C6H14N4O2	-1.55	Amino acid	KEGG	-3.0	-1.6	-2.3	-4.6	-2.3	-1.8
2	30	1.90	[M+H] ⁺	13104529	Asparagine	C4H8N2O3	-2.25	Amino acid	KEGG	-3.7	-2.3	-2.8	-3.8	-2.3	-2.1
2	85	23.64	[M+H] ⁺	609144470	Flavonoid di glycoside or (C12634), (C05625), (C17563)	C27H30O16	-2.72	Flavonoid	KEGG	-5.1	-4.4	-4.2	-5.9	-4.1	-3.2
2	84	23.63	[M+H] ⁺	61115847	Flavonoid di glycoside or (C05625), (C19796)	C27H30O16	-3.65	Flavonoid	KEGG	-7.3	-5.7	-7.8	-9.3	-4.7	-3.8
2	42	7.21	[M+H] ⁺	13805878	Gabaculine	C7H9NO2	-1.06	Benzoic acid	KEGG	-1.2	-1.1	1.0	-2.6	-2.6	-1.2
2	148	3.12	[M+H] ⁺	286138916	Glycylprolylhydroxyproline	C12H19N3O5	-2.90	Oligopeptide	HMDB	-2.6	-1.7	-1.2	-3.4	-2.3	-1.1
2	145	2.98	[M+H] ⁺	204087799	N-Acetyl-D-fucosamine	C8H15NO5	0.37	Monosaccharide	KEGG	-5.5	-4.7	-4.2	-8.6	-7.1	-5.4
2	28	2.95	[M+H] ⁺	188056519	N-Acetylglutamic acid	C7H11NO5	0.39	Glutamic acid	HMDB	-5.0	-3.8	-4.5	-5.3	-4.1	-3.7
2	26	7.80	[M+H] ⁺	203082779	Tryptophan	C11H12N2O2	0.76	Amino acid	KEGG	-3.3	-2.2	-2.5	-2.2	-2.0	-1.2
2	149	28.71	[M+H] ⁺	993208496	Zizyboeside II	C25H38O16	-0.38	Oligosaccharide	KEGG	-2.2	-1.9	-1.8	-3.2	-2.9	-2.3
3	170	21.27	[M+H] ⁺	278107025	2-Acetamido-3-hexylsulfanylpropanoic acid	C11H21NO5S	1.08		PubChem	1.1	-1.0	-1.0	-1.4	-1.3	-1.5
3	88	20.01	[M+H] ⁺	388074219	2-Methylbutyl glucosinolate	C12H22NO8S2	0.24	Aliphatic GLS	Metlin, KEGG	-2.1	-2.1	-1.5	-1.7	1.2	1.4
3	176	29.31	[M+H] ⁺	162094620	6-Methylthiohexanal doxime	C7H15NO5	-0.35		KEGG	-1.1	-1.1	-1.9	-2.5	-3.5	-1.8
3	92	10.13	[M+H] ⁺	466030487	Glucoberverin	C11H21NO8S3	-0.09	Aliphatic GLS	KEGG	-1.1	-1.2	1.5	3.9	1.9	1.6
3	93	23.98	[M+H] ⁺	422058563	Glucosasturtiin	C15H21NO8S2	0.09	Other GLS	KEGG	-1.4	-1.3	-1.2	1.7	1.7	1.7
3	94	15.94	[M+H] ⁺	408042725	Glucotropaeolin	C14H19NO8S2	-0.24	Other GLS	KEGG	1.0	-1.3	1.1	-1.4	-1.3	-1.2
3	7	2.00	[M+H] ⁺	146048587	Glutamic acid	C5H9NO4	-0.60	Amino acid	KEGG	1.8	1.4	1.7	2.1	1.4	1.4
3	13	4.25	[M+H] ⁺	235110428	Isoleucyl-Cysteine, Leucyl-Cysteine	C9H18NO3S5	-2.81	Dipeptide	HMDB	-2.5	-1.7	-1.1	1.1	1.1	1.2
3	53	3.31	[M+H] ⁺	286169876	Isovalerylcarnitine	C12H23NO4	-0.41	Carnitine	KEGG	-1.5	-1.4	-1.2	-1.1	-1.5	-1.2
3	80	20.47	[M+H] ⁺	947247457	Kaempferol 3-(2-feruloylsophoroside)	C38H48O24	1.23	Flavonoid	HMDB	1.0	-1.3	1.2	1.8	1.7	1.2
3	65	20.90	[M+H] ⁺	919249146	Kaempferol 3-O-[6-(4-coumaroyl)-beta-D-glucosyl-(1->2)-beta-D-glucosyl-(1->2)-beta-D-glucosyl-(1->2)-beta-D-glucoside]	C42H46O23	-1.23	Flavonoid	KEGG	-1.1	-1.5	-1.0	2.0	1.7	1.4
3	20.91	[M+H] ⁺	917235291	Kaempferol 3-O-[6-(4-coumaroyl)-beta-D-glucosyl-(1->2)-beta-D-glucosyl-(1->2)-beta-D-glucoside]	C42H46O23	-0.47	Flavonoid	KEGG	-1.2	-1.6	1.0	2.1	2.0	1.8	
3	17	2.96	[M+H] ⁺	263141815	Methionyl-Isoleucine	C11H22NO3S2	-2.18	Dipeptide	HMDB	-1.6	-1.6	-1.6	-1.3	-1.3	-1.2
3	112	33.28	[M+H] ⁺	385150146	Methylsyringin	C18H26O9	-0.68	Phenolic glycoside	HMDB	-1.4	-1.3	-1.3	-2.3	-2.0	-1.7
3	44	33.29	[M+H] ⁺	225111435	Olivetolic acid	C12H16O4	-3.29	Benzoic acid	KEGG	-1.6	-1.6	-1.5	-3.0	-2.2	-2.1
3	52	6.20	[M+H] ⁺	305087860	Starch acetate	C12H18O9	0.18	Carboxylic acid	HMDB	-1.2	-1.3	1.0	-1.0	-1.5	-1.0

Table S7. (Continued)

Cluster Mapping number	RT (m)	m/z	Mass (D)	Compound	Formula	ppm to DB	Classification	data base	Fold change					
									Coronato		Malibu			
									Pbg	Pbh	Pbr	Pbg	Pbh	Pbr
4	172	3.87	[M+H] ⁺	27698342	2-C-Methyl-D-erythritol 2,4-cyclodiphosphate	C5H12O9P2	-0.30	KEGG	-1.8	-1.1	-1.2	-1.6	-1.9	-2.2
4	33.64	[M+H] ⁺	33314561	3'-N'-Acetylflusarochromanone	C17H22N2O5	0.29	Benzopyran	HMDB	2.0	-1.0	1.8	-1.1	-1.1	1.3
4	165	43.28	[M+H] ⁺	62926168	Brassica napus non-flavonoid chlorophyll catabolite 3	C34H38N4O8	-0.05	Tetrapyrrole	HMDB	-4.3	-2.7	-4.0	-5.5	-5.7
4	61	16.87	[M+H] ⁺	380156128	cis-Zeaxtin-O-glucoside	C16H23N5O6	-3.67	Fattyacyl glycoside	KEGG	-2.0	-1.5	-1.5	-3.3	-2.8
4	35	12.05	[M+H] ⁺	222077301	Dioxacarb	C11H13NO4	0.35	Benzene	KEGG	-1.7	-1.3	-1.3	-1.7	-1.6
4	46	26.20	[M+H] ⁺	203056168	L-ascorbic acid ethyl ester	C8H12O6	0.22	Butenolide	metlin	-2.5	-1.5	-2.4	-11.8	-4.7
4	23	27.97	[M+H] ⁺	247107407	N-Acetyl-D-tryptophan	C13H14N2O3	-1.09	Amino acid	KEGG	-2.0	-1.8	-1.6	-1.8	-1.8
4	164	12.04	[M+H] ⁺	224091324	Salsolinol 1-carboxylate	C11H13NO4	-1.83	Quinoline	HMDB	-1.9	-1.5	-1.4	-2.1	-1.7
4	160	19.07	[M+H] ⁺	41191284	S-Furanopetasitin	C24H32O5S	3.51	Terpenoid	HMDB	-49.1	-5.3	-4.7	-2.0	-3.0
4	161	20.25	[M+H] ⁺	387200470	Sonehuonoside C	C19H30O8	-2.26	Terpenoid	HMDB	-1.7	-1.4	-1.4	-1.6	-1.5
4	24	4.14	[M+H] ⁺	384113953	Succinadenosine	C14H17N5O8	-2.70	Purine nucleoside	HMDB	-2.3	-1.6	-1.4	-2.0	-1.9
4	156	34.23	[M+H] ⁺	363075562	Sulfometuron methyl	C15H16N4O5S	-3.48	Sulfonylurea	KEGG	-3.0	-2.6	-3.3	-6.5	-3.2
5	36	17.69	[M+H] ⁺	329087708	1-O-Vanilloyl-beta-D-glucose	C14H18O9	-0.35	Phenolic glycoside	KEGG	-2.1	-1.7	-1.7	-1.6	-1.9
5	21	23.98	[M+H] ⁺	252085983	4-Hydroxy-3-methoxy-cinnamoylglycine	C12H13NO5	-2.75	Amino acid	KEGG	-1.6	-1.5	-1.3	1.0	-1.1
5	41	24.57	[M+H] ⁺	165019963	Formylsalicylic acid or (C14096), (C14100)	C8H6O4	0.24	Benzoic acid	KEGG	1.0	-1.2	1.1	-1.2	-1.0
5	20	23.98	[M+H] ⁺	206082062	N-Acetyl-L-phenylalanine	C11H13NO3	-0.79	Phenylalanine	KEGG, Metlin	-1.4	-1.3	-1.2	1.1	-1.1
5	155	27.17	[M+H] ⁺	349059875	Sulfometuron	C14H14N4O5S	-3.86	Sulfonylurea	KEGG	-1.2	-1.1	-1.0	-1.1	-1.3
7	63	23.89	[M+H] ⁺	225148117	(6S,9R)-Vomifolol	C13H20O3	-1.59	Fatty acyl glycoside	KEGG	1.7	1.5	1.5	1.6	1.4
7	120	21.34	[M+H] ⁺	335077667	5-O-Caffeoylshikimic acid	C16H16O8	1.32	Coumaric acid	Metlin, KEGG	4.8	4.5	5.3	3.9	2.7
7	72	33.14	[M+H] ⁺	571156250	Flavonoid-di-glycoside or (C16981), (C12628), (C12627)	C27H30O14	-0.13	Flavonoid	KEGG	2.4	2.2	3.2	2.2	2.5
7	147	4.77	[M+H] ⁺	375093384	Furanol 4-(6-malonylglucoside)	C15H20O11	0.26	O-Glycosyl comp.	HMDB	1.4	1.1	1.4	1.4	1.5
7	48	23.68	[M+H] ⁺	350088165	Indole-3-acetic-acid-O-glucuronide	C16H17NO8	0.07	O-Glucuronides	HMDB	6.4	1.8	3.3	3.1	1.9
7	67	17.00	[M+H] ⁺	963241943	Kaempferol 3-O-hydroxyferuloyl/sophoroside 7-O-glucoside	C43H48O25	1.27	Flavonoid	PubChem	1.5	1.2	1.6	2.7	1.9
7	163	20.31	[M+H] ⁺	371144623	Loganic acid	C16E24O10	1.19	Iridoid	KEGG	5.1	1.9	2.9	2.8	2.0
7	2.40	[M+H] ⁺	133014084	Malic acid	C4H6O5	-1.05	Hydroxy acid	KEGG	1.8	1.9	1.9	1.6	1.4	
8	59	23.68	[M+H] ⁺	323122986	Binapacryl	C15H18N2O6	-2.44	Dinoseb	KEGG	6.2	1.9	3.0	3.3	2.1
8	64	15.09	[M+H] ⁺	773210571	Kaempferol 3-sophorotrioside	C33H40O21	-3.76	Flavonoid	KEGG	6.7	4.9	6.4	12.9	9.4
9	124	39.91	[M+H] ⁺	929272949	2-Feruloyl-1,2'-disinapoylgentiobiose	C44H50O22	0.92	Phenylpropanoid	HMDB	1.1	-1.0	1.3	1.3	1.3
9	175	33.63	[M+H] ⁺	335159943	3'-N'-Acetylflusarochromanone	C17H22N2O5	-0.61	Benzopyran	HMDB	3.1	1.9	1.5	1.0	-1.3

Table S7. (Continued)

Cluster number	Mapping number	RT (m)	m/z	Mass (D)	Compound	Formula	Δ ppm to DB	Classification	data base	Fold change					
										Coronado		Malibu		Pbt	
11	153	21.46	[M+H] ⁺	551176697	(Z)-Resveratrol 3,4'-diglucoside	C ₂₆ H ₃₂ O ₁₃	-0.58	Stilbenoid	HMDB	1.7	1.6	2.0	2.0	1.7	1.6
11	132	18.43	[M+H] ⁺	355103210	1-Feruloyl-D-glucose	C ₁₆ H ₁₈ O ₉	-0.60	Phenylpropanoid	KEGG	1.8	1.6	1.8	2.1	1.7	1.6
11	37	26.28	[M+H] ⁺	415124878	2-Hydroxybenzaldehyde O-[xylosyl-(1->6)-glucoside]	C ₁₈ H ₂₄ O ₁₁	0.70	Phenolic glycoside	HMDB	3.0	2.3	3.2	2.7	1.8	1.9
11	125	43.09	[M+H] ⁺	299090393	3,4,5-Trimethoxycinnamic acid	C ₁₂ H ₁₄ O ₅	-4.20	Phenylpropanoid	HMDB	2.3	1.5	2.4	2.6	1.4	1.7
11	43	13.33	[M+H] ⁺	299075756	4-Hydroxybenzoate-O-glucoside	C ₁₃ H ₁₆ O ₈	1.18	Benzoic acid	KEGG	1.3	1.2	1.3	1.8	1.5	1.8
11	135	12.94	[M+H] ⁺	211059418	5-Hydroxyferulic acid methyl ester 1	C ₁₀ H ₁₀ O ₅	-3.12	Phenylpropanoid	KEGG	2.1	1.6	2.0	2.7	1.7	1.7
11	54	18.44	[M+H] ⁺	177054489	7-Methoxycoumarin or (C03081)	C ₁₀ H ₈ O ₃	-0.49	Coumarin	KEGG	2.0	1.9	1.9	2.6	1.7	1.7
11	38	12.10	[M+H] ⁺	138054703	Anthranilic acid	C ₇ H ₇ NO ₂	-1.98	Aromatic acid	KEGG	1.9	1.3	1.9	2.4	1.5	1.8
11	138	11.42	[M+H] ⁺	341087616	Caffeic acid 3-glucoside	C ₁₅ H ₁₈ O ₉	-0.61	Phenylpropanoid	KEGG	2.1	2.0	2.0	2.6	2.0	1.7
11	122	9.97	[M+H] ⁺	353087585	Chlorogenic acid	C ₁₆ H ₁₈ O ₉	-0.68	Phenylpropanoid	KEGG	2.3	1.7	2.4	2.0	1.7	1.5
11	9.92	[M+H] ⁺	355101624	Chlorogenic acid	C ₁₆ H ₁₈ O ₉	-2.12	Phenylpropanoid	KEGG	2.3	1.7	2.2	1.9	1.6	1.3	
11	15.86	[M+H] ⁺	353087616	Chlorogenic acid or Coumarin: (C01527) or (C08996)	C ₁₆ H ₁₈ O ₉	-0.59	Phenylpropanoid	KEGG	3.1	2.5	3.2	2.1	1.8	1.5	
11	123	15.81	[M+H] ⁺	355101654	Chlorogenic acid or Coumarin: (C01527) or (C08996)	C ₁₆ H ₁₈ O ₉	-2.03	Phenylpropanoid	KEGG	2.6	2.1	2.7	2.1	1.8	1.6
11	50	2.95	[M+H] ⁺	191019522	citric acid	C ₆ H ₈ O ₇	-0.85	Tricarboxylic acid	KEGG	3.9	2.7	3.5	3.4	2.4	2.7
11	136	12.93	[M+H] ⁺	371097992	Dihydroferulic acid 4-O-glucuronide	C ₁₆ H ₂₀ O ₁₀	-1.02	Phenylpropanoid	HMDB	2.4	1.8	2.1	2.9	1.9	2.0
11	133	18.43	[M+H] ⁺	195064651	Ferulic acid	C ₁₀ H ₁₀ O ₄	-2.69	Phenylpropanoid	KEGG	1.7	1.5	1.8	2.2	1.6	1.6
11	51	2.54	[M+H] ⁺	207014572	Garcinia acid	C ₆ H ₈ O ₈	-0.33	Carboxylic acid	HMDB	11.1	8.5	27.6	41.4	12.8	8.9
11	104	2.04	[M+H] ⁺	225061401	Glucosaminic acid	C ₇ H ₁₄ O ₈	-0.99	Glycoside	Metlin	4.9	3.0	4.1	6.2	3.2	2.9
11	68	26.16	[M+H] ⁺	725194081	Isoschaftoside 4'-glucoside or (HMDB40878)	C ₃₂ H ₄₈ O ₁₉	0.80	Flavonoid	HMDB	2.9	1.8	2.5	3.8	2.1	2.2
11	83	20.03	[M+H] ⁺	611159851	Kaempferol 3-O-beta-D-sophoroside or (C05625), (C17563)	C ₂₇ H ₃₀ O ₁₆	-1.35	Flavonoid	KEGG	1.2	1.1	1.4	1.6	1.5	1.4
11	81	20.46	[M+H] ⁺	949258301	Kaempferol tri glycoside + feruloyl	C ₆₈ H ₈₀ O ₂₄	-2.66	Flavonoid	HMDB	-1.0	-1.3	1.2	2.0	1.8	1.6
11	139	15.97	[M+H] ⁺	325092926	p-Coumaroyl-D-glucose or (C04415), (C05158)	C ₁₅ H ₁₈ O ₈	0.01	Phenylpropanoid	KEGG	2.3	2.0	2.7	4.0	4.1	2.3
11	140	15.99	[M+H] ⁺	165054881	Phenylpyruvic acid or (C12621), (C00811)	C ₉ H ₈ O ₃	0.03	Phenylpropanoid	KEGG	2.4	2.0	2.5	4.4	3.7	2.2
11	79	17.75	[M+H] ⁺	955242615	Quercetin 3-[p-coumaroyl-(1->6)-glucosyl-(1->2)-glucosyl-(1->2)-glucoside], Kaempferol 3-O-caffeoyl-sophoroside 7-O-glucoside	C ₄₂ H ₄₆ O ₂₄	-2.74	Flavonoid	HMDB	1.0	-1.2	1.1	2.3	1.9	1.8
11	69	29.93	[M+H] ⁺	799210444	Robinin	C ₃₃ H ₄₀ O ₁₉	1.38	Flavonoid	KEGG	2.3	1.8	2.4	1.8	1.3	1.6
11	57	12.94	[M+H] ⁺	193048950	Scopoletin, or (C10290), (C18077), (C01938)	C ₁₀ H ₈ O ₄	-3.24	Coumarin	KEGG	2.4	1.9	2.1	2.9	1.8	1.8
12	60	3.85	[M+H] ⁺	147066345	(S)-Mevalonic acid	C ₆ H ₁₂ O ₄	0.14	Hydroxy fatty acid	KEGG	2.1	2.0	2.3	1.7	1.6	1.3
12	137	13.27	[M+H] ⁺	341087585	1-Caffeoyl-beta-D-glucose or (C10431)	C ₁₅ H ₁₈ O ₉	-0.70	Phenylpropanoid	KEGG	2.4	2.1	2.1	3.0	2.3	2.1
12	131	23.26	[M+H] ⁺	195029892	3,4-Dihydroxyphenylpyruvate	C ₉ H ₈ O ₅	-0.16	Phenylpropanoid	KEGG	2.7	1.8	2.1	2.5	1.7	1.9
12	99	19.52	[M+H] ⁺	401109009	4-Hydroxy-5-(3',5'-dihydroxyphenyl)-valeric acid-O-glucuronide	C ₁₇ H ₂₀ O ₁₁	0.18	Glucuronide	HMDB	1.6	1.5	1.6	2.0	1.8	1.8

Table S7. (Continued)

Cluster number	Mapping number	RT (m)	m/z	Mass (D)	Compound	Formula	ppm to DB	Classification	data base	Fold change					
										Coronato		Malibu		Pbg	
12	74	22.70	[M+H] ⁺	341.13800	5-Deoxykiefvitone or (C09832), (C18023), (C09753), (C15510)	C20H20O5	-1.10	Flavonoid	KEGG	2.4	1.9	2.3	3.0	2.4	2.0
12	134	14.64	[M+H] ⁺	211.05949	5-Hydroxyferulic acid methyl ester II	C10H10O5	-2.83	Phenylpropanoid	KEGG	2.4	1.8	2.1	2.9	1.8	1.9
12	143	27.39	[M+H] ⁺	567.20786	Citrusin B	C27H36O13	-0.76	Phenylpropanoid	HMDB	2.6	1.8	2.7	2.3	1.9	1.9
12	55	27.40	[M+H] ⁺	219.101242	Eupatoriochromene	C13H14O3	-1.52	Coumarin	KEGG	2.6	1.7	2.4	2.0	1.5	1.6
12	82	20.06	[M+H] ⁺	609.145386	Flavonoid-di-glycoside or (C12634), (C05625), (C18942)	C27H30O16	-1.21	Flavonoid	KEGG	1.3	1.1	1.6	1.7	1.7	1.5
12	73	38.75	[M+H] ⁺	561.160889	Flavonol 3-O-beta-D-glucosyl-(1->2)-beta-D-glucoside	C27H30O13	-0.78	Flavonoid	KEGG	3.9	3.4	4.6	3.7	4.0	3.7
12	70	35.31	[M+H] ⁺	732.13989	Flavonol 3-O-beta-D-glucosyl-(1->2)-beta-D-glucosyl-(1->2)-beta-D-glucoside	C33H40O18	-0.32	Flavonoid	KEGG	2.2	1.9	2.5	2.0	1.9	1.8
12	71	38.58	[M+H] ⁺	723.213928	Flavonol 3-O-beta-D-glucosyl-(1->2)-beta-D-glucosyl-(1->2)-beta-D-glucoside tri glycoside	C33H40O18	-0.41	Flavonoid	KEGG	1.9	1.6	2.0	1.9	1.8	1.7
12	76	39.79	[M+H] ⁺	531.150269	Flavonol 3-O-D-xylosylglucoside	C26H28O12	-1.04	Flavonoid	KEGG	11.7	7.3	14.0	18.4	12.7	8.5
12	78	17.76	[M+H] ⁺	933.231506	Kaempferol 3-O-caffeoyl-sophoroside 7-O-glucoside/Quercetin 3-[p-coumaroyl-(->6)-glucosyl-(1->2)-glucosyl-(1->2)-glucoside]	C42H40O24	0.94	Flavonoid	HMDB	1.1	-1.1	1.2	2.4	2.1	1.9
12	56	33.73	[M+H] ⁺	325.091370	Mahaleboside	C15H16O8	-1.30	Coumarin	HMDB	3.2	2.8	3.7	5.0	5.3	4.2
12	75	34.36	[M+H] ⁺	517.134094	Medicarpin 3-O-glucoside-6'-malonate	C25H26O12	-1.99	Flavonoid	KEGG	26.1	18.8	30.3	28.1	24.0	15.0
12	121	38.74	[M+H] ⁺	399.106934	p-Coumaroyl quinic acid	C16H18O8	-1.60	Phenylpropanoid	KEGG	3.5	3.0	4.2	3.8	3.7	3.0
12	141	33.28	[M+H] ⁺	487.125000	Phymarolin I	C24H24O11	0.77	Lignan	KEGG	13.1	3.8	8.4	67.3	48.7	20.0
12	77	33.75	[M+H] ⁺	547.145325	Puerarin xyloside	C26H28O13	-0.73	Flavonoid	KEGG	3.5	2.9	4.2	4.4	4.5	3.7
12	150	22.62	[M+H] ⁺	135045029	Simple phenolic or (C05613), (C07086), (C07215) or (C01454)	C8H8O2	-0.70	Phenolica acid	KEGG	3.4	2.2	2.3	2.3	1.7	1.7
13	119	37.81	[M+H] ⁺	591.171875	1,2-Bis-O-sinapoyl-beta-D-glucoside	C28H20O14	-0.08	Phenylpropanoid	KEGG	1.4	1.3	1.8	-1.4	-1.1	-1.0
13	154	31.87	[M+H] ⁺	469.080780	Resveratrol-sulfoglucoside	C20H20O15	-0.48	Stilbenoid	Metlin, HMDB	1.2	3.7	4.9	1.8	1.7	2.5

Table S8. *Paraburkholderia* species-mediated changes in shoot semi-polar secondary metabolites (LC-MS) in two Broccoli cultivars (Coronado and Malibu) at 11 dpi. The tabulated data corresponds to the hierarchical cluster analysis (HCA) shown in **Fig 4b2** of the manuscript. The fold change corresponding to each metabolites was calculated by dividing the abundance of each metabolites in Paraburkholderia treated plants to the non-treated control. *Pbg*: *Paraburkholderia graminis*, *Pbh*: *P. hospita*, and *Pbt*: *P. terricola*.

Cluster Mapping number	RT(m)	m/z	Mass(D)	Compound	Formula	ppm to DB	Classification	data base	Fold change						
									Coronado			Malibu			
									<i>Pbg</i>	<i>Pbh</i>	<i>Pbt</i>	<i>Pbg</i>	<i>Pbh</i>	<i>Pbt</i>	
1	64	15.09	[M+H] ⁺	773210571	Kaempferol 3-sophorotrioside	C33H40O21	-3.76	Flavonoid	KEGG	3.5	4.4	6.3	22.8	22.6	16.0
1	118	23.80	[M+H] ⁺	488238007	N1,N10-Dicoumaroyl spermidine	C25H31N3O4	-1.66	Phenylpropanoid	HMDB	-1.1	-1.7	1.0	10.7	2.3	5.3
1	156	34.23	[M+H] ⁺	363075562	Sulfometuron methyl	C15H16N4O6S	-3.48	sulfonyleurea	KEGG	-1.6	1.0	-1.5	1.2	1.4	6.9
2	153	21.46	[M+H] ⁺	551176697	(Z)-Resveratrol 3,4-diglucoside	C26H32O13	-0.58	Stilbenoid	HMDB	1.6	1.7	1.6	1.7	1.8	2.2
2	125	43.09	[M+H] ⁺	299090393	3,4,5-Trimethoxycinnamic acid	C12H14O5	-4.20	Phenylpropanoid	HMDB	3.1	2.8	3.3	7.9	5.7	7.6
2	120	21.34	[M+H] ⁺	355077667	5-O-Caffeoylshikimic acid	C16H16O8	1.32	Phenylpropanoid	Metlin, KEGG	7.4	7.5	7.8	8.5	7.7	7.4
2	38	12.10	[M+H] ⁺	1380584703	Anthranilic acid	C7H7NO2	-1.98	aromatic acid	KEGG	1.9	1.8	2.1	3.4	2.9	4.8
2	50	2.95	[M+H] ⁺	191019562	citric acid	C6H8O7	-0.85	Carboxylic acid	KEGG	2.2	2.9	3.3	4.8	5.4	6.1
2	2.40	[M+H] ⁺	133014084	Malic acid	C4H6O5	-1.05	Hydroxy acid	KEGG	1.6	1.4	2.0	2.3	2.3	2.4	
2	154	31.87	[M+H] ⁺	469080780	Resveratrol-sulfoglucoside	C20H20O15	-0.48	Stilbenoid	Metlin, HMDB	1.8	1.1	1.6	1.6	1.7	2.9
3	134	14.64	[M+H] ⁺	211059479	5-Hydroxyferulic acid methyl ester II	C10H10O5	-2.83	Phenylpropanoid	KEGG	4.2	4.4	3.5	6.8	5.2	4.7
3	59	23.68	[M+H] ⁺	323122986	Binapacryl	C15H18N2O6	-2.44	Dinoseb	KEGG	7.0	6.9	7.8	10.3	7.9	8.7
3	48	23.68	[M+H] ⁺	350088165	Indole-3-acetic-acid-O-glucuronide	C16H17NO8	0.07	o-glucuronides	HMDB	5.8	5.9	6.2	10.8	6.7	10.1
4	63	23.89	[M+H] ⁺	225148117	(6S,9R)-Vomifoliol	C13H20O3	-1.59	Fattyacyl glycoside	KEGG	2.4	2.6	2.2	2.9	2.6	2.8
4	60	3.85	[M+H] ⁺	147066345	(S)-Mevalonic acid	C6H12O4	0.14	Hydroxy fatty acid	KEGG	-1.1	1.2	1.2	1.6	2.0	1.6
4	137	13.27	[M+H] ⁺	341087585	1-Caffeoyl-beta-D-glucose or (C10431)	C15H18O9	-0.70	Phenylpropanoid	KEGG	3.0	4.2	2.8	5.9	4.8	4.1
4	132	18.43	[M+H] ⁺	355103210	1-Feruloyl-D-glucose	C16H20O9	-0.60	Phenylpropanoid	KEGG	2.1	2.4	2.1	3.6	3.1	3.0
4	124	39.91	[M+H] ⁺	929272949	2-Feruloyl-1,2-disinapoylgentiobiose	C44H50O22	0.92	Phenylpropanoid	HMDB	1.4	1.5	1.8	2.9	2.3	2.7
4	37	26.28	[M+H] ⁺	415124878	2-Hydroxybenzaldehyde O-[xylosyl-(1->6)-glucoside]	C18H24O11	0.70	Phenolic glycoside	HMDB	3.0	4.6	4.2	5.4	4.6	5.1
4	131	23.26	[M+H] ⁺	195102982	3,4-Dihydroxyphenylpyruvate	C9H8O5	-0.16	Phenylpropanoid	KEGG	2.2	3.8	2.8	3.7	3.5	5.8
4	74	22.70	[M+H] ⁺	341138000	5-Deoxykivitone or (C09832), (C18023), (C09753), (C15510)	C20H20O5	-1.10	Flavonoid	KEGG	3.5	3.4	3.5	6.8	5.7	4.4
4	135	12.94	[M+H] ⁺	211059418	5-Hydroxyferulic acid methyl ester I	C10H10O5	-3.12	Phenylpropanoid	KEGG	2.7	2.9	2.7	5.7	4.3	4.3
4	54	18.44	[M+H] ⁺	177058489	7-Methoxycoumarin or (C03081)	C10H8O3	-0.49	Coumarin	KEGG	2.4	2.8	2.6	4.0	3.9	3.2
4	138	11.42	[M+H] ⁺	341087616	Caffeic acid 3-glucoside	C15H18O9	-0.61	Phenylpropanoid	KEGG	2.4	3.0	2.5	5.1	4.4	4.0
4	9.92	[M+H] ⁺	355101624	Chlorogenic acid	C16H18O9	-2.12	Phenylpropanoid	KEGG	2.8	3.0	3.0	4.5	3.4	3.8	
4	122	9.97	[M+H] ⁺	353087585	Chlorogenic acid	C16H18O9	-0.68	Phenylpropanoid	KEGG	2.8	3.0	2.9	4.3	3.2	4.0

Table S8. (Continued)

Cluster number	Mapping number	Rf(m)	m/z	Mass(D)	Compound	Formula	ppm to DB	Classification	data base	Fold change							
										Coronato		Malibu		Coronato		Malibu	
										Pbg	Pht	Pbg	Pht	Pbg	Pht	Pbg	Pht
4	123	15.81	[M+H] ⁺	355.101654	Chlorogenic acid or Coumarin: (C01527) or (C08996)	C16H18O9	-2.03	Phenylpropanoid	KEGG	2.7	3.4	2.7	3.5	2.8	3.6		
4	15.86	[M+H] ⁺	353.087616	Chlorogenic acid or Coumarin: (C01527) or (C08996)	C16H18O9	-0.59	Phenylpropanoid	KEGG	2.8	3.5	2.9	3.6	2.8	3.9			
4	143	27.39	[M+H] ⁺	567.207886	Citrinin B	C27H36O13	-0.76	Phenylpropanoid	HMDB	4.3	4.5	5.3	4.6	3.5	4.0		
4	136	12.93	[M+H] ⁺	371.097992	Dihydroferulic acid 4-O-glucuronide	C16H20O10	-1.02	Phenylpropanoid	HMDB	3.0	3.3	3.1	6.6	5.0	5.4		
4	55	27.40	[M+H] ⁺	219.101242	Eupatoriocromene	C13H14O3	-1.52	Coumarin	KEGG	4.3	3.7	4.8	5.0	3.9	3.9		
4	133	18.43	[M+H] ⁺	195.064651	Ferulic acid	C10H10O4	-2.69	Phenylpropanoid	KEGG	2.2	2.4	2.1	3.6	3.1	2.8		
4	82	20.06	[M+H] ⁺	691.045886	Flavonoid-di-glycoside (C12634) or (C05625), (C18942)	C27H30O16	-1.21	Flavonoid	KEGG	1.7	1.8	2.2	4.4	4.2	3.9		
4	72	33.14	[M+H] ⁺	571.156250	Flavonoid-di-glycoside (C16981) or (C12628), (C12627)	C27H30O14	-0.13	Flavonoid	KEGG	4.9	5.5	7.0	19.1	17.7	14.9		
4	73	38.75	[M+H] ⁺	561.160889	Flavonol 3-O-beta-D-glucosyl-(1->2)-beta-D-glucoside	C27H30O13	-0.78	Flavonoid	KEGG	6.7	8.3	10.3	16.0	18.2	12.8		
4	70	35.31	[M+H] ⁺	723.21989	Flavonol 3-O-beta-D-glucosyl-(1->2)-beta-D-glucosyl-(1->2)-beta-D-glucoside	C33H40O18	-0.32	Flavonoid	KEGG	2.6	2.8	3.0	4.5	4.1	4.2		
4	71	38.58	[M+H] ⁺	723.21988	Flavonol 3-O-beta-D-glucosyl-(1->2)-beta-D-glucosyl-(1->2)-beta-D-glucoside tri glycoside	C33H40O18	-0.41	Flavonoid	KEGG	2.5	2.8	2.4	3.2	2.8	2.5		
4	76	39.79	[M+H] ⁺	531.150269	Flavonol 3-O-D-xylosylglucoside	C28H28O12	-1.04	Flavonoid	KEGG	12.1	35.8	47.3	127.5	119.5	96.3		
4	104	2.04	[M+H] ⁺	225.061401	Glucosheptonic acid	C7H14O8	-0.99	Glycoside	Metlin	2.0	2.6	3.1	6.3	5.9	4.4		
4	68	26.16	[M+H] ⁺	725.194081	Isoschaftoside 4'-glucoside or Schaftoside 4'-glucoside	C32H38O19	0.80	Flavonoid	HMDB	4.7	5.6	5.4	13.1	7.4	10.5		
4	80	20.47	[M+H] ⁺	947.247437	Kaempferol 3-(2-feruloylsophoroside) 7-glycoside	C43H48O24	1.23	Flavonoid	HMDB	1.2	1.5	1.6	3.6	3.1	2.9		
4	65	20.90	[M+H] ⁺	919.249146	Kaempferol 3-O-[6-(4-coumaroyl)-beta-D-glucosyl-(1->2)-beta-D-glucosyl-(1->2)-beta-D-glucoside]	C62H46O23	-1.23	Flavonoid	KEGG	1.1	1.0	1.4	4.3	4.3	2.8		
4	20.91	[M+H] ⁺	917.235291	Kaempferol 3-O-[6-(4-coumaroyl)-beta-D-glucosyl-(1->2)-beta-D-glucosyl-(1->2)-beta-D-glucoside]	C62H46O23	-0.47	Flavonoid	KEGG	1.0	1.1	1.3	4.5	4.8	3.4			
4	83	20.03	[M+H] ⁺	611.159851	Kaempferol 3-O-beta-D-sophoroside or (C05625), (C17563)	C27H30O16	-1.35	Flavonoid	KEGG	2.1	1.9	2.5	4.3	3.9	3.6		
4	78	17.76	[M+H] ⁺	933.231506	Kaempferol 3-O-caffeoyl-sophoroside 7-O-glucoside or (HMDB37938)	C42H46O24	0.94	Flavonoid	HMDB	1.1	1.4	1.5	5.2	4.9	4.5		
4	67	17.00	[M+H] ⁺	963.241943	Kaempferol 3-O-hydroxyferuloylsophoroside 7-O-glucoside	C43H48O25	1.27	Flavonoid	PubChem	1.6	2.3	2.3	5.4	4.4	4.9		
4	81	20.46	[M+H] ⁺	949.258301	Kaempferol tri glycoside + feruloyl	C63H48O24	-2.66	Flavonoid	HMDB	1.3	1.5	1.7	2.8	3.1	3.0		
4	56	33.73	[M+H] ⁺	325.091370	Mahaleboside	C15H16O8	-1.30	Coumarin	HMDB	4.5	5.8	9.8	40.6	46.2	22.5		
4	75	34.36	[M+H] ⁺	571.134094	Medicarpin 3-O-glucoside-6'-malonate	C25H26O12	-1.99	Flavonoid	KEGG	7.5	38.7	59.3	476.8	401.1	264.0		
4	121	38.74	[M+H] ⁺	391.06954	p-Coumaroyl quinic acid	C16H18O8	-1.60	Phenylpropanoid	KEGG	6.3	6.9	9.9	15.4	17.1	11.4		
4	77	33.75	[M+H] ⁺	547.145325	Puerarin xyloside	C28H28O13	-0.73	Flavonoid	KEGG	5.2	9.6	11.8	27.6	27.4	20.6		
4	79	17.75	[M+H] ⁺	955.245615	Quercetin 3-[p-coumaroyl-(4->6)-glucosyl-(1->2)-glucosyl-(1->2)-glucoside], Kaempferol 3-O-caffeoyl-sophoroside 7-O-glucoside	C62H46O24	-2.74	Flavonoid	HMDB	1.2	1.5	1.7	4.8	3.6	3.9		
4	69	29.93	[M+H] ⁺	792.210144	Robinin	C33H40O19	1.38	Flavonoid	KEGG	2.9	3.0	3.2	4.5	3.4	4.5		
4	57	12.94	[M+H] ⁺	193.048950	Scopoletin or (C10290), (C18077), (C01938)	C10H8O4	-3.24	Coumarin	KEGG	3.1	3.3	3.3	7.4	5.5	5.4		



Table S8. (Continued)

Cluster Mapping number	RT(m)	m/z	Mass(D)	Compound	Formula	Δ ppm to DB	Classification	data base	Fold change						
									Coronado		Malibu		Pbt		Pbh
									Pbg	Pbh	Pbt	Pbg	Pbh	Pbt	
4	150	22.62	[M+H] ⁺	135048029	Benzyl formate or (C07086), (C07215) or (C01454)	C8H8O2	-0.70	Phenolic acids	KEGG	2.6	4.5	2.9	3.1	3.2	4.6
5	119	37.81	[M+H] ⁺	591171875	1,2-Bis-O-sinapoyl-beta-D-glucoside	C28H20O4	-0.08	Phenylpropanoid	KEGG	2.3	1.8	2.5	2.7	2.9	2.9
5	175	33.63	[M+H] ⁺	335159943	3'-N'-Acetylflusarochromanone	C17H22N2O5	-0.61	Benzopyran	HMDB	17.2	4.5	11.5	7.5	6.4	2.8
5	33.64	[M+H] ⁺		333145691	3'-N'-Acetylflusarochromanone	C17H22N2O5	0.29	Benzopyran	HMDB	16.8	4.7	10.7	5.9	4.0	2.9
5	99	19.52	[M+H] ⁺	401109009	4-Hydroxy-5-(3',5'-dihydroxyphenyl)-valeric acid-O-glucuronide	C17H22O11	0.18	Citricuronic acid	HMDB	2.2	2.4	1.7	2.4	2.2	1.9
5	147	4.77	[M+H] ⁺	375093384	Furanol 4-(6-malonylglucoside)	C15H20O11	0.26	o-glycosyl comp.	HMDB	1.5	1.3	1.5	2.6	2.2	1.9
5	93	23.98	[M+H] ⁺	422058563	Glucanasturtiin	C15H24NO8S2	0.09	other GLS	KEGG	-1.2	-1.1	-1.3	4.7	6.4	2.5
5	163	20.31	[M+H] ⁺	371144623	Loganic acid	C16H24O10	1.19	Iridoid	KEGG	16.6	10.7	11.5	21.0	20.1	12.0
7	21	23.98	[M+H] ⁺	252085983	4-Hydroxy-3-methoxy-cinnamoylglycine	C12H13NO5	-2.75	Amino acid	KEGG	-1.8	-2.2	-2.0	-1.9	-1.9	-1.1
7	148	3.12	[M+H] ⁺	286138916	Glycylprolylhydroxyproline	C12H19N3O5	-2.90	Oligopeptides	HMDB	-1.2	-1.9	-1.4	-1.6	-2.3	-1.0
7	20	23.98	[M+H] ⁺	206082062	N-Acetyl-L-phenylalanine	C11H13NO3	-0.79	Phenylalanine	KEGG, Metlin	-1.9	-2.1	-1.9	-2.0	-2.0	-1.2
7	158	19.33	[M+H] ⁺	178035156	Sulforaphane	C6H11NO2	-1.83	Sulfoxides	HMDB	-17.3	-2.9	-2.8	-12.0	-8.4	-1.7
8	165	43.28	[M+H] ⁺	629261688	Brassica napus non-fluorescent chlorophyll catabolite 3	C34H58N4O8	-0.05	Tetrapyrrole	HMDB	-11.2	-10.9	-11.0	-29.9	-37.4	-6.8
9	36	17.69	[M+H] ⁺	329087708	1-O-Vanilloyl-beta-D-glucose	C14H18O9	-0.35	Benzoic acid	KEGG	-6.0	-4.8	-3.7	-5.9	-4.7	-2.2
9	61	16.87	[M+H] ⁺	380156128	cis-Zeaxtin-O-glucoside	C16H23NO6	-3.67	Fatty acyl glycoside	KEGG	-3.5	-3.3	-3.1	-7.2	-6.1	-2.5
9	35	12.05	[M+H] ⁺	222077301	Dioxaacarb	C11H13NO4	0.35	Benzenes	KEGG	-2.6	-2.6	-2.7	-3.9	-3.1	-1.7
9	85	23.64	[M+H] ⁺	609144470	Flavonoid di glycoside (C12634) or (C05625), (C17563), (C19796)	C27H30O16	-2.72	Flavonoid	KEGG	-6.1	-6.4	-6.9	-18.6	-17.6	-4.4
9	84	23.63	[M+H] ⁺	611158447	Flavonoid di glycoside (C12634) or (C05625), (C17563), (C19796)	C27H30O16	-3.65	Flavonoid	KEGG	-5.4	-5.8	-6.4	-13.8	-15.1	-3.0
9	42	7.21	[M+H] ⁺	138058678	Gabaculine	C7H9NO2	-1.06	Benzoic acid	KEGG	-3.5	-2.6	-2.6	-4.7	-5.4	-1.2
9	23	27.97	[M+H] ⁺	247107407	N-Acetyl-D-tryptophan	C13H14N2O3	-1.09	Amino acid	KEGG	-3.0	-3.1	-3.7	-3.8	-3.9	-1.6
9	44	33.29	[M+H] ⁺	255111435	Olivetolic acid	C12H16O4	-3.29	Benzoic derivative	KEGG	-2.2	-2.2	-2.1	-4.0	-5.4	-1.9
9	164	12.04	[M+H] ⁺	224091324	Salsolinol 1-carboxylate	C11H13NO4	-1.83	Quinoline	HMDB	-2.5	-2.5	-2.6	-3.4	-3.1	-1.6
9	160	19.07	[M+H] ⁺	481191284	S-Furanopetasitin	C24H32O5S	3.51	Terpenoid	HMDB	-2.2	-2.1	-2.6	-2.2	-3.2	1.1
9	161	20.25	[M+H] ⁺	387200470	Sonehuonioside C	C19H30O8	-2.26	Terpenoid	HMDB	-1.7	-1.8	-1.9	-1.9	-2.1	-1.1
9	24	4.14	[M+H] ⁺	384113953	Succinyladenosine	C14H17N5O8	-2.70	Purine nucleoside	HMDB	-3.1	-2.2	-2.2	-3.1	-2.5	-1.4
9	155	27.17	[M+H] ⁺	349108675	Sulfometuron	C14H14N4O5S	-3.86	Sulfonylurea	KEGG	-1.7	-1.8	-1.5	-1.9	-2.2	-1.1
9	26	7.80	[M+H] ⁺	203082779	tryptophan	C11H12N2O2	0.76	Amino acid	KEGG	-1.6	-2.9	-2.0	-3.9	-4.9	-2.3
9	149	28.71	[M+H] ⁺	593208496	Zizyboside II	C25H38O16	-0.38	Oligosaccharides	KEGG	-2.6	-3.2	-2.8	-5.1	-5.3	-2.2
10	3.00	[M+H] ⁺		114054932	1-Pyrroline-2-carboxylic acid	C5H7NO2	-0.39	Pyrrones	HMDB	-1091.0	-1044.4	-1099.5	-1494.1	-1572.9	-1495.0
10	172	3.87	[M+H] ⁺	276988342	2-C-Methyl-D-erythritol 2,4-cyclodiphosphate	C5H12O9P2	-0.30	KEGG	KEGG	-4.3	-2.7	-3.8	-8.0	-4.6	-1.7
10	111	20.19	[M+H] ⁺	556176819	4-Demethylismondasin 2-(E)-ferulate	C25H31NO12	-0.99	Phenylpropanoid	HMDB	-2.3	-2.0	-1.9	-3.1	-3.0	-1.4
10	29	1.63	[M+H] ⁺	175118820	Arginine	C6H14N4O2	-0.89	Amino acid	KEGG	-3.0	-2.5	-2.4	-6.7	-5.2	-3.1

Table S8. (Continued)

Cluster Mapping number	Rf(m)	m/z	Mass(D)	Compound	Formula	ppm to DB	Classification	data base	Fold change					
									Coronato		Malibu		Pbg	
10	1.80	[M+H] ⁺	173.104156	Arginine	C6H14N4O2	-1.55	Amino acid	KEGG	-2.9	-2.5	-2.2	-8.1	-5.4	-4.0
10	30	[M+H] ⁺	131.045929	Asparagine	C4H8N2O3	-2.25	Amino acid	KEGG	-2.9	-2.7	-4.3	-4.0	-4.9	
10	112	[M+H] ⁺	385.150146	Methylsyringin	C18H26O9	-0.68	Phenylpropanoid	HMDB	-2.1	-1.9	-3.2	-4.2	-1.6	
10	145	[M+H] ⁺	204.087799	N-Acetyl-D-fucosamine	C8H15NO5	0.37	Monosaccharide	KEGG	-4.6	-6.2	-6.6	-8.4	-8.0	-5.3
10	28	[M+H] ⁺	188.056519	N-Acetylglutamic acid	C7H13NO5	0.39	Glutamic acid	HMDB	-4.0	-5.3	-4.8	-9.2	-7.2	-7.4
10	34	[M+H] ⁺	161.968781	Raphanusamic acid	C4H5NO2S2	-0.88	Alpha amino acid	Metlin, HMDB	-1.6	-2.0	-1.7	-3.4	-2.7	-2.0
10	52	[M+H] ⁺	305.087800	Starch acetate	C12H18O9	0.18	Carboxylic acid	HMDB	-3.0	-2.9	-2.4	-2.2	-2.0	1.0
10	33	[M+H] ⁺	247.111847	Valyl-Methionine/ Methionyl-Valine	C10H20N2O3S	-1.38	Dipeptide	HMDB	-3.1	-2.5	-2.3	-8.7	-3.8	-2.8
11	170	[M+H] ⁺	278.107025	2-acetamido-3-hexylsulfonylpropanoic acid	C11H21NO3S	1.08		PubChem	-1.5	-1.5	-1.6	-2.2	-1.9	-1.3
11	88	[M+H] ⁺	388.074219	2-Methylbutyl glucosinolate	C12H23NO8S2	0.24	Aliphatic GLS	Metlin, KEGG	-2.2	-1.7	-2.0	-2.4	-2.2	-1.2
11	157	[M+H] ⁺	164.019562	3-Methylsulfanylpropyl isothiocyanate	C5H9NO6S2	-1.64	Sulfoxide	HMDB	-5.3	-2.2	-2.8	-3.8	-4.7	-1.4
11	176	[M+H] ⁺	162.094620	6-Methylthiohexanaldoxime	C7H15NO5	-0.35		KEGG	-1.7	-1.7	-2.9	-1.7	-2.0	1.7
11	92	[M+H] ⁺	406.030487	glucoiberberin	C11H21NO6S3	-0.09	Aliphatic GLS	KEGG	-1.4	-1.6	-1.0	2.1	3.2	2.1
11	13	[M+H] ⁺	255.110428	Isoleucyl-Cysteine, Leucyl-Cysteine	C9H18N2O3S	-2.81	Dipeptide	HMDB	-2.6	-2.0	-1.8	-1.3	-1.7	1.1
11	53	[M+H] ⁺	246.169876	Isovalerylcarnitine	C12H23NO4	-0.41	Carnitine	KEGG	-1.5	-1.8	-1.5	-2.0	-1.7	-1.0
11	17	[M+H] ⁺	263.141815	Methionyl-Isoleucine	C11H22N2O3S	-2.18	Dipeptide	HMDB	-3.3	-1.9	-2.7	-1.4	-1.9	1.2
14	41	[M+H] ⁺	165.019363	Formylsalicylic acid or (C14100)	C8H6O4	0.24	Benzoic acid	KEGG	4.4	2.2	2.4	1.3	1.2	-1.3
14	7	[M+H] ⁺	146.045837	Glutamic acid	C5H9NO4	-0.60	Amino acid	KEGG	1.6	1.8	1.9	2.3	2.4	1.8

Table S9. Polar primary and semi-polar secondary metabolites classes and their metabolites ID used in Fig 6 of the manuscript. GC: Gas chromatography- mass spectrometry, LC: Liquid chromatography- mass spectrometry.

Mapping #	Compound	Tool
Amino acid		
1	Serine	GC
2	Threonine	GC
3	Valine	LC
4	L-Aspartic acid	GC
5	ASPARTIC ACID-TRITMS	GC
6	Glutamic acid	GC
7	Glutaminic acid	LC
8	Putrescine	GC
9	Tryptophan or (C07839), (C14916)	LC
10	Isoleucine	GC
11	Proline	GC
12	Glutamine	GC
13	Isoleucyl-Cysteine	LC
14	5-Hydroxyindoleacetylglucine	LC
15	L-Asparagine	GC
16	GABA	GC
17	Methionyl-Isoleucine	LC
18	L-5-Oxoproline	GC
19	L-Serine	GC
20	N-Acetyl-L-phenylalanine	LC
21	4-Hydroxy-3-methoxy-cinnamoylglucine	LC
22	Glycine	GC
23	N-Acetyl-D-tryptophan	LC
24	Succinyladenosine	LC
25	L-Phenylalanine	GC
26	tryptophan	LC
27	Ornithine	GC
28	N-Acetylglutamic acid	LC
29	Arginine	LC
30	Asparagine	LC
31	Lysine	GC
32	Methionine	GC
33	Valyl-Methionine	LC
34	Raphanusamic acid	LC
Benzene, Benzoic acid		
35	Dioxacarb	LC
36	1-O-Vanilloyl-beta-D-glucose	LC
37	2-Hydroxybenzaldehyde O-[xylosyl-(1->6)-glucoside]	LC
38	Anthranilic acid	LC
39	Apiosylglucosyl 4-hydroxybenzoate	LC
40	dihydroxybenzoic acid glucoside	LC
41	Formylsalicylic acid	LC
42	Gabaculine	LC
43	4-Hydroxybenzoate-O-glucoside	LC
44	Olivetolic acid	LC
Butenolide		
45	Ascorbic acid	GC
46	L-ascorbic acid ethyl ester	LC
Carboxylic acid		
47	Malic acid	GC
48	Indole-3-acetic-acid-O-glucuronide	LC

Mapping #	Compound	Tool
49	Indole-3-acetaldehyde or (C10663), (C06345)	LC
50	Citric acid	LC
51	Garcinia acid	LC
52	Starch acetate	LC
Carnitines		
53	Isovalerylcarnitine	LC
Coumarin		
54	7-Methoxycoumarin or (C03081)	LC
55	Eupatoriochromene	LC
56	Mahaleboside	LC
57	Scopoletin or (C10290), (C18077), (C01938)	LC
Ester		
58	Phosphoenolpyruvate	GC
59	Binapacryl	LC
Fatty acid, Fatty acyl glycoside		
60	(S)-Mevalonic acid	LC
61	cis-Zeatin-O-glucoside	LC
62	Ethyl 7-epi-12-hydroxyjasmonate glucoside	LC
63	(6S,9R)-Vomifoliol	LC
Flavonoid		
64	Kaempferol 3-sophorotrioxide	LC
65	Kaempferol 3-O-[6-(4-coumaroyl)-beta-D-glucosyl-(1->2)-beta-D-glucosyl-(1->2)-beta-D-glucoside]	LC
66	Kaempferol 3-(2'''-sinapoylsophoroside) 7-glucoside	LC
67	Kaempferol 3-O-hydroxyferuloylsophoroside 7-O-glucoside	LC
68	Isoschaftoside 4'-glucoside/ Schaftoside 4'-glucoside	LC
69	Robinin	LC
70	Flavonol 3-O-beta-D-glucosyl-(1->2)-beta-D-glucosyl-(1->2)-beta-D-glucoside	LC
71	Flavonol 3-O-beta-D-glucosyl-(1->2)-beta-D-glucosyl-(1->2)-beta-D-glucoside tri glycoside	LC
72	Flavonoid-di-glycoside Kaempferitrin (C16981)/ Vitexin 2''-rhamnoside (C12628)/ Apigenin 7-O-neohesperidoside (C12627)	LC
73	Flavonol 3-O-beta-D-glucosyl-(1->2)-beta-D-glucoside	LC
74	5-Deoxykiveton/ 6-Prenylaringenin (C09832)/ Flavaprenin (C18023)/ Glepidotin B (C09753)/ 4-Glyceollidin (C15510)	LC
75	Medicarpin 3-O-glucoside-6'-malonate	LC
76	Flavonol 3-O-D-xylosylglucoside	LC
77	Puerarin xyloside	LC
78	Kaempferol 3-O-caffeoylsophoroside 7-O-glucoside/ Quercetin 3-[p-coumaroyl-(->6)-glucosyl-(1->2)-glucosyl-(1->2)-glucoside]	LC

Table S9. (Continued)

Mapping #	Compound	Tool
79	Quercetin 3-[p-coumaroyl-(→6)-glucosyl-(1→2)-glucosyl-(1→2)-glucoside], Kaempferol 3-O-caffeoyl-sophoroside 7-O-glucoside	LC
80	Kaempferol 3-(2-feruloylsophoroside) 7-glucoside	LC
81	Kaempferol tri glycoside + feruloyl	LC
82	Flavonoid-di-glycoside:(C12634) or (C05625), (C18942)	LC
83	Kaempferol 3-O-beta-D-sophoroside or (C05625), (C17563)	LC
84	Flavonoid di glycoside: (C12634) or (C05625), (C17563), (C19796)	LC
85	Flavonoid di glycoside: (C12634) or (C05625), (C17563), (C19796)	LC
Glucosinolate		
86	Glucoraphanin	LC
87	hexyl glucosinolate (3-Methylpentyl glucosinolate/ 4-Methylpentyl glucosinolate)	LC
88	2-Methylbutyl glucosinolate	LC
89	4-Methylthiobutyl-desulfoglucosinolate	LC
90	Glucosylsyringic acid	LC
91	Glucosylsyringic acid	LC
92	Glucosylsyringic acid	LC
93	Glucosylsyringic acid	LC
94	Glucosylsyringic acid	LC
95	4-Hydroxyglucobrassicin	LC
96	4-methoxyglucobrassicin	LC
97	Desulfoglucobrassicin	LC
98	Glucobrassicin	LC
Glucuronide		
99	4-Hydroxy-5-(3',5'-dihydroxyphenyl)-valeric acid-O-glucuronide	LC
Glycoside		
100	D-(-)-Fructofuranose, pentakis(trimethylsilyl) ether (isomer 1)	GC
101	D-(-)-Fructopyranose	GC
102	Xylose	GC
103	Glucose	GC
104	Glucoheptonic acid	LC
105	Fructose	GC
106	Sorbose	GC
107	D-Galactopyranoside, methyl 2,3,4-tris-O-(trimethylsilyl)-, acetate	GC
108	d-Galactose, 2,3,4,5,6-pentakis-O-(trimethylsilyl)-, o-methylxyme, (1E)-	GC
109	Myo-Inositol	GC
110	Sucrose	GC
Hydroxycinnamate		
111	4-Demethylsimmondsin 2'-(E)-ferulate	LC
112	Methylsyringic acid	LC
113	Sinapic acid	LC
114	5-O-Feruloylquinic acid	LC
115	6-Feruloylglucose 2,3,4-trihydroxy-3-methylbutylglycoside	LC
116	3-O-Caffeoyl-4-O-methylquinic acid	LC
117	O-Feruloylquinic acid	LC

Mapping #	Compound	Tool
118	N1,N10-Dicoumaroylspermidine	LC
119	1,2-Bis-O-sinapoyl-beta-D-glucoside	LC
120	5-O-Caffeoylsinapic acid	LC
121	p-Coumaroyl quinic acid	LC
122	Chlorogenic acid	LC
123	Chlorogenic acid or Coumarin: (C01527) or (C08996)	LC
124	2-Feruloyl-1,2'-disinapoylgentiobiose	LC
125	3,4,5-Trimethoxycinnamic acid	LC
126	Urolithin A-3-O-glucuronide	LC
127	1,2,2'-Trisinapoylgentiobioside	LC
128	3',6'-Disinapoylsucrose	LC
129	1-O-Sinapoyl beta-D-glucoside or 4-O-beta-D-Glucosyl-sinapate	LC
130	Sinapic acid	LC
131	3,4-Dihydroxyphenylpyruvate	LC
132	1-Feruloyl-D-glucose	LC
133	Ferulic acid	LC
134	5-Hydroxyferulic acid methyl ester II	LC
135	5-Hydroxyferulic acid methyl ester I	LC
136	Dihydroferulic acid 4-O-glucuronide	LC
137	1-Caffeoyl-beta-D-glucose or (C10431)	LC
138	Caffeic acid 3-glucoside	LC
139	p-Coumaroyl-D-glucose or (C04415), (C05158)	LC
140	Phenylpyruvic acid or (C12621), (C00811)	LC
Lignan		
141	Phymarolin I	LC
142	Syringin	LC
143	Citrusin B	LC
Methoxyphenol		
144	4-Heptyloxyphenol	LC
Monosaccharide		
145	N-Acetyl-D-fucosamine	LC
Organic acid		
146	Mannonic acid, lactone	GC
O-glycosyl compound		
147	Furanol 4-(6-malonylglucoside)	LC
Oligopeptide		
148	Glycylprolylhydroxyproline	LC
Oligosaccharide		
149	Zizyboside II	LC
Phenolic acid		
150	Simple phenolic: (C05613) or (C07086), (C07215), (C01454)	LC
Quinoline		
151	Quinoline	LC
Saccharide		
152	(3S,7E,9S)-9-Hydroxy-4,7-megastigmadien-3-one 9-glucoside	LC
Stilbenoid		
153	(Z)-Resveratrol 3,4'-diglucoside	LC
154	Resveratrol-sulfoglucoside	LC
Sulfonylurea		
155	Sulfometuron	LC
156	Sulfometuron methyl	LC

Table S9. (Continued)

Mapping #	Compound	Tool
Sulfoxide		
157	3-Methylsulfinylpropyl isothiocyanate	LC
158	Sulforaphane	LC
Terpenoid		
159	(4R,5S,7R,11S)-11,12-Dihydroxy-1(10)-spirovetiven-2-one 11-glucoside	LC
160	S-Furanopetasitin	LC
161	Sonchuionoside C	LC
162	10-Deoxygeniposidic acid	LC
163	Loganic acid	LC
Others		
164	Salsolinol 1-carboxylate	LC
165	Brassica napus non-fluorescent chlorophyll catabolite 3	LC
166	1-Methyl-4-(1-methyl-2-propenyl)-benzene/ alpha-Ionene/ 1,2,3,4-Tetrahydro-1,5,7-trimethylnaphthalene/ 5,7alpha-Dihydro-1,4,4,7a-tetramethyl-4H-indene	LC
167	2-(3-Phenylpropyl)tetrahydrofuran	LC
168	2,5-Dihydro-2,4,5-trimethyloxazole/ 2-Acetylpyrrolidine	LC
169	2,6-Dimethoxy-4-propylphenol	LC
170	2-acetamido-3-hexylsulfonylpropanoic acid	LC
171	2-Amino-2-deoxyisochorismate	LC
172	2-C-Methyl-D-erythritol 2,4-cyclodiphosphate	LC
173	O-Demethylpuromycin	LC
174	pantothenic acid (vitamin B5)	LC
175	3'-N'-Acetylfusarochromanone	LC
176	6-Methylthiohexanaldoxime	LC